FUSE

Fungal Systematics and Evolution

VOLUME 17
JUNE 2026
PAGES 124–150

doi.org/10.15761/fuse.2026.17.08

Integrative assessment of *Panaeolus* and *Psilocybe* species (*Agaricales, Basidiomycota*) from Uruguay: multigene phylogenetic analyses, psychoactive alkaloid content, and novel taxonomic insights

G. Morera[1,2]*, G. Robledo[3,4,5], S. Martínez-Kopp[6], L. Rodríguez[2,7], G. Hernández Dossi[2,7,8], I. Carrera[2,7], S. Lupo[1]*

[1]Instituto de Biología, Sección Micología, Facultad de Ciencias-Universidad de la República, Iguá 4225, Montevideo 11400, Uruguay
[2]Arché-Núcleo Interdisciplinario de Estudios sobre Psicodélicos-Espacio Interdisciplinario-Universidad de la República, José Enrique Rodó 1843, Montevideo 11200, Uruguay
[3]CeTBIO-Centro de Transferencia de Bioinsumos, Facultad de Ciencias Agropecuarias-Universidad Nacional de Córdoba, Ing. Agr. Félix Aldo Marrone 746, CP 5000 Córdoba, Argentina
[4]CONICET, Consejo Nacional de Investigaciones Científicas y Técnicas, Buenos Aires, Argentina
[5]Fundación FungiCosmos, Córdoba, Argentina
[6]Laboratorio de Patología Vegetal-INIA Treinta y Tres, Ruta 8 Km 281, 33000 Treinta y Tres, Uruguay
[7]Laboratorio de Síntesis Orgánica, Departamento de Química Orgánica, Facultad de Química-Universidad de la República, Av. General Flores 2124, Montevideo 11800, Uruguay
[8]Laboratorio de Resonancia Magnética Nuclear, Departamento de Química Orgánica, Facultad de Química-Universidad de la República, Av. General Flores 2124, Montevideo 11800, Uruguay

*Corresponding authors: G. Morera: mguillemorera@gmail.com, S. Lupo: slupo@fcien.edu.uy

Keywords:
Coprophilous fungi, hallucinogenic fungi, indol alkaloids, psilocin, psilocybin, secotioid mushrooms

Abstract: Coprophilous species of *Panaeolus* and *Psilocybe* are ecologically significant components of dung-associated fungal communities worldwide and include the principal natural producers of the psychoactive alkaloids psilocybin (PSB) and psilocin (PS). Despite their relevance, the diversity of these genera in Uruguay has remained poorly documented. In this study, we conducted an integrative assessment of Uruguayan specimens using multigene phylogenetic analyses, detailed morphological characterization, and quantitative alkaloid profiling. Seven species were confirmed. Five species of *Panaeolus* were identified: *Pa. antillarum*, *Pa. cyanescens*, *Pa. foenisecii*, *Pa. retirugis*, and *Pa. charrua sp. nov.* All species, except *Pa. antillarum*, represent new records for Uruguay, and *Pa. charrua* is described here as a species new to science. Two species of *Psilocybe* were documented: *Ps. cubensis*, previously recorded for Uruguay, and *Ps. stuntzii*, representing a new record for Uruguay and an extension of its known distribution range. Quantitative NMR analyses revealed detectable PSB and/or PS exclusively in *Pa. cyanescens*, *Ps. cubensis*, and *Ps. stuntzii*, with *Ps. cubensis* exhibiting the highest alkaloid concentrations. This study substantially expands the known diversity of coprophilous agarics in Uruguay, provides the first integrative taxonomic framework for these genera in the country, and contributes novel chemical data relevant to both systematics and regulatory contexts.

Citation: Morera G, Robledo G, Martínez-Kopp S, Rodríguez L, Hernández G, Carrera I, S. Lupo (2026). Integrative assessment of *Panaeolus* and *Psilocybe* species (Agaricales, Basidiomycota) from Uruguay: multigene phylogenetic analyses, psychoactive alkaloid content, and novel taxonomic insights. *Fungal Systematics and Evolution* **17**: 124–150. doi: 10.15761/fuse.2026.17.08
Received: 4 February 2026; **Accepted:** 29 April 2026; **Effectively published online:** 12 June 2026
Corresponding editor: P.W. Crous

INTRODUCTION

Coprophilous fungi play a key role in ecosystems by contributing to the degradation of cellulose and other polymers that are partially or completely digested by herbivores (Richardson 2001). They exhibit specific adaptations to this habitat, including tolerance to dehydration, resistance to UV radiation, and the ability of basidiospores to survive passage through the digestive tract of herbivores (Garnica *et al.* 2007). The introduction of domestic livestock into the Americas in the 15th century (Primo 1992), followed by its dispersal across South America and successive reintroductions of breeds from Asia, North America, and Europe, greatly increased the availability of dung. These conditions likely facilitated the establishment of coprophilous fungi through both the introduction of non-native species—co-introduced with livestock—and the expansion or substrate shift of native taxa. As a result, the geographic origins of many dung-associated fungi remain difficult to determine, with some lineages suggesting recent introductions, as hypothesized for *Bolbitiaceae* species in the Americas (e.g., Morera *et al*. 2024) and *P. cubensis* in Australia (McTaggart *et al.* 2023); whereas others may have been present in America prior to livestock arrival and later expanded with domesticated animals, as proposed for *P. cubensis* (Bradshaw *et al*. 2026). Consequently, dung-rich environments may host a mixture of native and introduced lineages, including taxa previously undescribed and new to science.

The most conspicuous basidiomata-forming taxa of coprophilous fungi belong to the order *Agaricales* (*Basidiomycota*) and are distributed across several genera, including *Bolbitius, Conocybe, Coprinellus, Deconica, Agrocybe,*

Panaeolus, Pholiotina, Psathyrella, Psilocybe, and *Stropharia* (Dix & Webster 1995, Ramírez-Cruz *et al*. 2013, Strauss *et al*. 2022). These fungi can exhibit either an agaricoid habit, in which the pileus expands to expose the lamellae at maturity, or a secotioid habit, in which the lamellae remain enclosed at maturity. Several species within these genera are known to produce psychoactive alkaloids, mainly psilocybin (PSB) and psilocin (PS). The PSB biosynthetic pathways appear to have been evolutionarily conserved as a result of complex evolutionary processes which implies natural selection, convergent evolution and horizontal gene transfer (Meyer & Slot 2023, Schäfer *et al*. 2025). When PSB is dephosphorylated, it produces PS, a serotonin (5-HT2A) receptor partial agonist that targets the animal central nervous system and is responsible for the psychoactive effects observed in humans (Halberstadt & Geyer 2011, Plazas & Faraone 2023). Species of *Panaeolus* and *Psilocybe* comprise most of the known dung-associated psychoactive fungi, with total alkaloid contents (PSB + PS) ranging from 1.5 to 3 % of dry mass (Guzmán *et al*. 1998, Allen 2010, Laussmann & Meier-Giebing 2010, Gotvaldová *et al*. 2022, Batista *et al*. 2025).

Both *Panaeolus* and *Psilocybe* species have been historically used by diverse cultures for medicinal, religious, and spiritual purposes (Wasson 1957, Ott 1993). More recently, PSB has gained attention in biomedicine due to promising results in treating depression and other psychiatric conditions (Carhart-Harris *et al*. 2021, Haikazian *et al.* 2023). Ongoing U.S. FDA–approved phase II clinical trials are testing PSB-assisted therapy for major depressive disorder (Raison 2019, Højlund *et al*. 2025). In this context, the effects of administration of whole mushrooms in clinical trials have not been fully elucidated; however, recent preclinical studies suggest that they may differ from those of pure PSB, likely due to the contribution of other metabolites acting synergistically (Zhuk *et al.* 2015, Dörner *et al.* 2022). Yet, outside the clinical framework, the popular use of these fungi is largely supported by domestic cultivation and wild harvesting (Batista *et al.* 2025). In such cases, identification is often based on the characteristic bluing reaction of the pileus or stipe when damaged (Lenz *et al.* 2020).

The taxonomic history of *Panaeolus* and *Psilocybe* dates back to the first half of the 19th century, when both were treated as infrageneric taxa within *Agaricus* (Fries 1821, 1836–1838, 1849). They were subsequently elevated to genus rank by Kummer (1871) and Quélet (1872), respectively. Today, *Panaeolus* comprises approximately 56 species and *Psilocybe* around 150 species, ranging from agaricoid to secotioid forms, which grow on dung, decaying wood, or soil across temperate, tropical, and desert regions worldwide (Ramírez-Cruz *et al.* 2013, Strauss *et al.* 2022, Voto & Angelini 2024, Consiglio & Marchetti 2025, He *et al.* 2026*)*. Both genera have been previously studied in the region, with several species recorded in neighboring countries. In Argentina and Brazil, for example, 17 species of *Panaeolus* and 29 of *Psilocybe* have been reported (Guzmán 2005, Niveiro & Albertó 2012, Silva 2013, Van Court *et al*. 2022, Strauss *et al*. 2023, Batista *et al.* 2025). In Uruguay, knowledge of *Panaeolus* and *Psilocybe* remains limited. To date, the following species have been recorded: *Panaeolus antillarum* (Gerhardt 1996, Sequeira 2017), *Pa. acuminatus* (Rosa-Mato 1939, Felippone 1928), *Pa. papilionaceus* (Herter 1907, Felippone 1928, Rosa-Mato 1939), *Pa. semiovatus* (as *Pa. phalaenarum*, Felippone 1928), *Psilocybe caeruleoannulata* Singer ex Guzmán (Guzmán 1978), *Ps. uruguayensis* Singer ex Guzmán (Guzmán 1978), *Ps. cubensis* (Sequeira 2013), and *Ps. bullacea* (Felippone 1928). Documenting the diversity of these genera in Uruguay is important both, from a taxonomic perspective and due to their relevance as the main natural producers of PSB, particularly in the context of emerging regulations concerning fungi and their derivatives.

The aim of this study was to analyze the diversity of coprophilous fungi of the genera *Panaeolus* and *Psilocybe* in Uruguay using phylogenetic and morphological approaches, to provide detailed morphological descriptions and to determine the content of the main psychoactive alkaloids (PSB and PS) in the species.

MATERIALS AND METHODS

Sampling

During sampling campaigns conducted in Uruguay between 2021 and 2024 to document coprophilous agaric fungi, surveys were carried out in cattle- and horse-grazed fields across the southern and eastern regions of the country (departments of Montevideo, Colonia, Maldonado, Lavalleja, Rocha, Tacuarembó and Cerro Largo). Basidiomata collected in the field were placed in aluminum-foil envelopes for transport to the laboratory. Tissue samples were aseptically taken for DNA analysis, and basidiomata were subsequently air-dried at 20 °C. Part of the sample was separated for chemical analysis, kept at ≈ 20 °C degrees in darkness, and a representative sample was deposited in the MVHC Herbarium ("Montevideo, Humanidades y Ciencias"). In two cases, anonymous spore-print donations identified as *Ps. cubensis* were received (MVHC 5762 and MVHC 5764); these were cultivated to obtain basidiomata, following the procedure described in Rodríguez *et al.* (2025).

Morphological analysis

Macro- and micromorphological studies of the basidiomata were conducted following the terminology and methodology of previous authors (Singer 1960, Guzman & Petrarca 1972, Young 1989, Gerhardt 1996, Wright & Albertó 2002, Malysheva *et al.* 2019, Voto & Angelini 2024, Batista *et al.* 2025). For each species, we elaborated descriptions covering both macroscopic and microscopic characters. Macroscopic assessments emphasized texture, color following Kornerup & Wanscher (1978), and the dimensions of the pileus, margin, context, lamellae, and stipe. Microscopic structures were examined with a light microscope; small sections of basidiomata were rehydrated in KOH (5 %) and stained with Congo Red (1 %), as needed. Images were captured using an AmScope digital microscope camera. Sections of pileus, lamellae, and stipe were analyzed, and measurements were taken for n = 30 elements of each structure, including: basidiospores, basidia, and cystidia (length × width). Basidiospore dimensions are reported as (a–)b–c(–d), where b–c represents 90 % of the measured values and the extremes (a, d) are given in brackets. The basidiospore length-to-width ratio (Q) and its mean value (Q_m) were also calculated.

Molecular protocols

Genomic DNA extraction was performed from basidiomata tissue fragments following a standard CTAB protocol (Doyle & Doyle 1987) and stored at –20 °C. The ITS and LSU regions were amplified with primers ITS4/ITS5 or ITS1F/ITS4B (White *et al.* 1990) and LR0R/LR5 or LR0R/LR7 (Vilgalys & Hester 1990), respectively. For *Psilocybe* specimens, the *rpb1* region was also amplified with primers Rpb1-af/Rpb1-cr (Matheny *et al.* 2002). PCR reactions contained 2 µL of genomic DNA (~60 ng), 16 µL of ultrapure water, 0.25 µL of Taq polymerase (1 U), 0.5 µL of each primer (10 mM), 0.7 µL of 50 mM $MgCl_2$, 2.5 µL of dNTPs (2.5 mM), and 2.5 µL of 10× buffer, in a final volume of 25 µL. Amplifications were performed in a MultiGene Optimax thermocycler (Labnet International Inc.) under the following conditions: initial denaturation at 94 °C for 3 min; 35 cycles of 94 °C for 60 s, 50 °C for 45 s, and 72 °C for 60 s; followed by a final extension at 72 °C for 5 min. PCR products were verified by electrophoresis on 1% agarose gels in TBE buffer, stained with EZ-Vision One (Amresco®), and visualized under UV light. The purified PCR products were sent to Macrogen (Seoul, Korea) for sequencing. The received sequences were inspected and edited with Bioedit v. 7.0.5.3 (Hall *et al.* 1999) and finally deposited in GenBank (Tables S1, S2).

Phylogenetic analysis

To explore the phylogenetic relationships of *Panaeolus* and *Psilocybe* species, two data sets were constructed, one for each genus, combining the new DNA sequences generated in the present work with sequences retrieved from GenBank (NCBI). Scientific names and GenBank Accession Numbers of sequences are listed in Tables S1 and S2. The *Panaeolus* dataset was composed of ITS and LSU sequences, and *Staktophyllus* was selected as an outgroup (Voto & Angelini 2024, Consiglio & Marchetti 2025). The *Psilocybe* dataset was composed of ITS, LSU, *rpb1* and *tef1* sequences, and *Deconica* was selected as an outgroup (Ramirez-Cruz *et al.* 2013). For each dataset, each region (ITS, LSU, *rpb1* and *tef1*) was individually aligned using the MAFFT online service (Katoh *et al.* 2019) using the G-INS-I alignment method. All obtained alignments were manually inspected and adjusted with Bioedit.

The best-fit partitioning strategy and the best-fit model of nucleotide evolution for each dataset was estimated using ModelFinder (Kalyaanamoorthy *et al.* 2017) implemented in the IQ-Tree software (Nguyen *et al.* 2015) with 4 data blocks for *Panaeolus* dataset (ITS1; 5.8S; ITS2; and LSU) and 12 data blocks for *Psilocybe* dataset (ITS1; 5.8S; ITS2; and LSU; *rpb1* 1st, 2nd, and 3rd codon positions; *rpb1* introns; *tef1* 1st, 2nd, and 3rd codon positions; and *tef1* introns), restricting the models to those implemented using MrBayes v. 3.2. (Ronquist *et al.* 2012).

Bayesian inference and maximum likelihood phylogenetic analyses were performed independently to each concatenated dataset using the partition scheme and evolutionary models defined in ModelFinder following Robledo *et al.* (2020, 2021). BI was performed in MrBayes v. 3.2 (Ronquist *et al.* 2012) using the CIPRES science gateway (Miller *et al.* 2010; http://www.phylo.org/). Two independent runs were performed, each one starting from random trees with four simultaneous independent chains, for 10 M generations, sampling parameters every 1000 generations. The burn-in tree discard value was set at 0.25, and remaining trees were used to reconstruct a 50 % majority rule consensus tree and calculate Bayesian posterior probabilities (BPP) of the clades. ML searches were performed in IQ-TREE, with 100 ML initial searches, starting from one randomized stepwise addition parsimony tree. Branch support (BS) was calculated using UFBoot (ultrafast bootstrap approximation implemented in IQ-TREE with 1000 replications) (Hoang *et al*. 2018). A node was considered strongly supported with BPP ≥ 0.95 and/or BS ≥ 95 % (Hyde *et al.* 2013, Minh *et al.* 2020). Alignments and phylogenetic trees are available at Zenodo (DOI: 10.5281/zenodo.18852023).

Chemical analysis

For quantitative analyses of PSB and PS, extracts were prepared following Rodríguez *et al.* (2025). Briefly, 0.3 g of a pooled mixture of fruiting bodies (stipe + pileus) were ground, then divided in 3 Falcon tubes and subjected to four consecutive extractions with 1.7 mL methanol under sonication for 30 min (25–30 °C). Solvents were combined and removed by vacuum evaporation to obtain dry extracts, which were redissolved in 0.6 mL DMSO-d_6 for quantitative Nuclear Magnetic Resonance (qNMR) analyses on a Bruker Avance Neo 400 spectrometer. qNMR analyses were carried out using the PULse Length based CONcentration (PULCON) method, which allows the determination of the absolute content of target compounds. ^{1}H-NMR was used for the quantification of PS and ^{31}P-NMR for PSB. Data were expressed as the percentage of PSB or PS by dry mass. Samples were analyzed in triplicate, and results are presented as mean ± relative standard deviation (RSD). However, in cases where only a single measurement was possible, the corresponding value is reported without an error estimation (Table 1). Finally, we systematically reviewed the literature to document whether each species represented in the phylogenetic analysis had previously been reported as producing PSB and/or PS. For this purpose, we assigned presence or absence to each species in the phylogeny (Figs 1, 2) based on the previously published data (Guzmán & Petrarca 1972, Høiland 1978, Young 1989, Guzman *et al.* 1998, Senn-Irlet *et al.* 1999, Allen 2010, Guzman *et al*. 2012, Borovicka *et al.* 2012, Hyde 2014, Borovicka *et al.* 2015, Wang & Tzean 2015, Li *et al.* 2020, Nkadimeng *et al.* 2020, Voto & Angelini 2021, Gotvaldová *et al.* 2022, Strauss *et al*. 2023, Allen *et al*. 2024, Canan *et al.* 2024, Ostuni *et al.* 2024, and the references within).

RESULTS

Phylogenetic analysis

The concatenated *Panaeolus* dataset consisted of 285 sequences (including the outgroup) and 1695 aligned positions including gaps. Within the ITS region (772 bp), 170 sites were parsimony-informative, 61 were singleton, and 541 were constant, while in the LSU region (923 bp), 47 sites were parsimony-informative, 46 were singleton, and 830 were con-

Table 1. Psilocybin (PSB) and psilocin (PS) content expressed as percentage of dry mass in samples of *Panaeolus* and *Psilocybe* species collected in Uruguay.

Species	Voucher or sample	%PSB	%PS
Panaeolus antillarum	MVHC 5787	<LOD	<LOD
Panaeolus charrua	MVHC 5825	<LOD	<LOD
Panaeolus charrua	MVHC 5833	<LOD	<LOD
Panaeolus cyanescens	MVHC 5827	<LOD	<LOD
Panaeolus cyanescens	MVHC 5839	<LOQ	0.06 ± 0.01
Panaeolus cyanescens	MVHC 5842a	0.09	0.2
Panaeolus cyanescens	MVHC 5879	0.28 ± 0.019	0.31 ± 0.035
Panaeolus cyanescens	MVHC 5880	0.04 ± 0.009	0.11 ± 0.009
Panaeolus cyanescens	PC_sample 2[a]	0.03	0.28
Panaeolus cyanescens	PC_sample 3[a]	<LOD	0.42
Panaeolus cyanescens	PC_sample 4[a]	<LOD	0.31
Panaeolus foenisecii	MVHC 5862	<LOD	<LOD
Panaeolus retirugis	MVHC 5797	<LOD	<LOD
Panaeolus retirugis	MVHC 5863	<LOD	<LOD
Psilocybe cubensis	MVHC 5762	<LOD	0.32 ± 0.007
Psilocybe cubensis	MVHC 5849 Sample 1[a]	0.71	0. 209
Psilocybe cubensis	MVHC 5849 Sample 2	<LOD	0.066 ± 0.006
Psilocybe cubensis	MVHC 5849 Sample 3	0.44 ± 0.019	<LOQ
Psilocybe cubensis	MVHC 5850	0.41 ± 0.011	0.22 ± 0.016
Psilocybe cubensis	MVHC 5851	<LOD	0.26 ± 0.006
Psilocybe cubensis	MVHC 5853	0.052 ± 0.009	0.077 ± 0.012
Psilocybe stuntzii	MVHC 5854	<LOD	<LOQ
Psilocybe stuntzii	MVHC 5866	<LOD	<LOD
Psilocybe stuntzii	PU_sample 1	<LOD	<LOQ
Psilocybe stuntzii	PU_sample 2	<LOD	<LOQ

PC and PU samples correspond to pools of basidiomata without associated voucher. For triplicate samples, results are presented as mean ± relative standard deviation (RSD). a: Only a single measurement (n = 1) was possible due to limited sample availability; therefore, the corresponding value is reported without an error estimate. LOD (Limit of detection): 0.017% PS and 0.013% PSB; LOQ (Limit of quantification): 0.034% PS and 0.036% PSB (Rodriguez et al. 2025).

stant. The partitions and evolutionary models selected were: ITS1 + ITS2 (HKY+F+G4), 5.8S + LSU (K2P+I+G4). Maximum Likelihood and Bayesian Inference analyses resulted in highly similar topologies. The ML tree is shown in Figure 1 and has been divided into three panels to facilitate visualization of the major clades and terminal lineages. Nine major clades (A–I in Fig. 1) were consistently recovered, most of them with high support in both analyses (BPP ≥ 0.95 and/or BS ≥ 95 %), indicating stable relationships among the principal lineages of *Panaeolus*. A total of 57 sequences generated in this study were clustered within five species: *Panaeolus antillarum* (BPP: 1, BS: 100), *Pa. cyanescens* (BPP: 1, BS: 99), *Pa. foenisecii* (BPP: 1, BS: 99), *Pa. retirugis* (BPP: 0.98, BS: 98) and an isolated clade *Pa. charrua sp. nov.* (BPP: 1, BS: 98). The *Psilocybe* combined dataset comprised 228 terminals and 3560 total aligned positions including gaps (including the outgroup). ITS region contained 720 bp with 241 parsimony-informative sites, 37 singleton, and 442 constant; LSU region 875 bp with 60 parsimony-informative, 50 singleton, and 765 constant; *rpb1* region 1412 bp with 601 parsimony-informative, 216 singleton, and 595 constant; and *tef1* region 553 bp with 183 parsimony-informative, 25 singleton, and 344 constant. The partitions and evolutionary models selected were: ITS1 + ITS2 + *rpb1* 2ndpos (HKY+F+I+G4), 5.8S + *tef1* 1stpos + *tef1* 3rdpos (SYM+I), LSU (K2P+I+G4), *rpb1* 1stpos (F81+F+G4), *rpb1* 3rdpos (HKY+F+G4), *rpb1* introns (HKY+F+G4), *tef1* 2nd-pos (GTR+F+I) and *tef1* introns (HKY+F+I). The phylogenetic trees obtained from ML and BI analyses using the combined data sets showed overall the same topology. The ML tree is shown in Fig. 2 and has been divided into two panels to facilitate visualization of the major clades and terminal lineages. The global tree is divided into two large strongly supported clades (1–2), each with two well-defined clades (A-D) (Fig. 2). Sequences corresponding to 16 Uruguayan samples were clustered in two clades: *Psilocybe cubensis* (BPP:0.77, BS:83) and *Ps. stuntzii* BPP:0.97, BS:83).

Chemical analysis

Quantification of psilocybin (PSB) and psilocin (PS) by qNMR was performed on 25 extracts derived from pooled specimens representing each of the seven species recorded in Uruguay (Table 1): *Pa. antillarum*, *Pa. cyanescens*, *Pa. foenisecii*, *Pa. charrua*, *Pa. retirugis*, *Ps. cubensis*, and *Ps. stuntzii*. Psilocibin was quantified by ^{1}H-NMR using the signal at 6.27 ppm (H-5 of the indole ring), whereas PSB was quantified by ^{31}P-NMR targeting the phosphate resonance at -2.875 ppm. The values obtained for each species are summarized in Table 1. Only three species showed significant PS or PSB contents: *Ps. stuntzii* showed detectable levels of PS but below the quantification limits, *Pa. cyanescens* displayed moderate alkaloid concentrations (PSB up to 0.28 %; PS up to 0.42 %) and *Ps. cubensis* yielded the highest overall contents (PSB up to 0.71 %; PS up to 0.32 %).

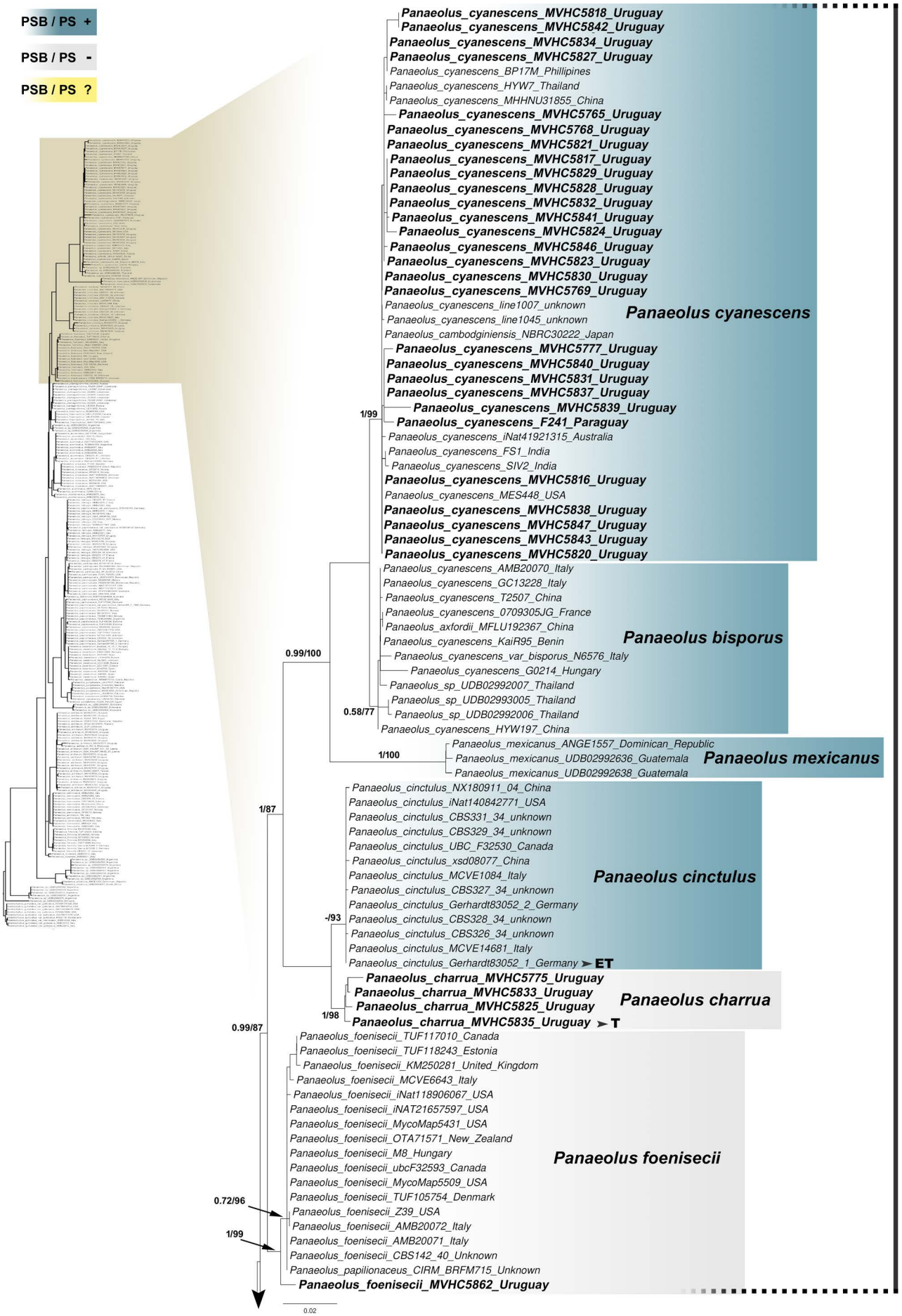
PSB / PS +
PSB / PS -
PSB / PS ?
Panaeolus_cyanescens_MVHC5818_Uruguay
Panaeolus_cyanescens_MVHC5842_Uruguay
Panaeolus_cyanescens_MVHC5834_Uruguay
Panaeolus_cyanescens_MVHC5827_Uruguay
Panaeolus_cyanescens_BP17M_Phillipines
Panaeolus_cyanescens_HYW7_Thailand
Panaeolus_cyanescens_MHHNU31855_China
Panaeolus_cyanescens_MVHC5765_Uruguay
Panaeolus_cyanescens_MVHC5768_Uruguay
Panaeolus_cyanescens_MVHC5821_Uruguay
Panaeolus_cyanescens_MVHC5817_Uruguay
Panaeolus_cyanescens_MVHC5829_Uruguay
Panaeolus_cyanescens_MVHC5828_Uruguay
Panaeolus_cyanescens_MVHC5832_Uruguay
Panaeolus_cyanescens_MVHC5841_Uruguay
Panaeolus_cyanescens_MVHC5824_Uruguay
Panaeolus_cyanescens_MVHC5846_Uruguay
Panaeolus_cyanescens_MVHC5823_Uruguay
Panaeolus_cyanescens_MVHC5830_Uruguay
Panaeolus_cyanescens_MVHC5769_Uruguay
Panaeolus_cyanescens_line1007_unknown
Panaeolus_cyanescens_line1045_unknown
Panaeolus_cambodginiensis_NBRC30222_Japan
Panaeolus_cyanescens_MVHC5777_Uruguay
Panaeolus_cyanescens_MVHC5840_Uruguay
Panaeolus_cyanescens_MVHC5831_Uruguay
Panaeolus_cyanescens_MVHC5837_Uruguay
Panaeolus_cyanescens_MVHC5839_Uruguay
Panaeolus_cyanescens_F241_Paraguay
Panaeolus_cyanescens_iNat41921315_Australia
Panaeolus_cyanescens_FS1_India
Panaeolus_cyanescens_SIV2_India
Panaeolus_cyanescens_MVHC5816_Uruguay
Panaeolus_cyanescens_MES448_USA
Panaeolus_cyanescens_MVHC5838_Uruguay
Panaeolus_cyanescens_MVHC5847_Uruguay
Panaeolus_cyanescens_MVHC5843_Uruguay
Panaeolus_cyanescens_MVHC5820_Uruguay
Panaeolus cyanescens
1/99
Panaeolus_cyanescens_AMB20070_Italy
Panaeolus_cyanescens_GC13228_Italy
Panaeolus_cyanescens_T2507_China
Panaeolus_cyanescens_0709305JG_France
Panaeolus_axfordii_MFLU192367_China
Panaeolus_cyanescens_KaiR95_Benin
Panaeolus_cyanescens_var_bisporus_N6576_Italy
Panaeolus_cyanescens_G0214_Hungary
Panaeolus_sp_UDB02992007_Thailand
Panaeolus_sp_UDB02993005_Thailand
Panaeolus_sp_UDB02992006_Thailand
Panaeolus_cyanescens_HYW197_China
Panaeolus bisporus
0.99/100
0.58/77
Panaeolus_mexicanus_ANGE1557_Dominican_Republic
Panaeolus_mexicanus_UDB02992636_Guatemala
Panaeolus_mexicanus_UDB02992638_Guatemala
Panaeolus mexicanus
1/100
Panaeolus_cinctulus_NX180911_04_China
Panaeolus_cinctulus_iNat140842771_USA
Panaeolus_cinctulus_CBS331_34_unknown
Panaeolus_cinctulus_CBS329_34_unknown
Panaeolus_cinctulus_UBC_F32530_Canada
Panaeolus_cinctulus_xsd08077_China
Panaeolus_cinctulus_MCVE1084_Italy
Panaeolus_cinctulus_CBS327_34_unknown
Panaeolus_cinctulus_Gerhardt83052_2_Germany
Panaeolus_cinctulus_CBS328_34_unknown
Panaeolus_cinctulus_CBS326_34_unknown
Panaeolus_cinctulus_MCVE14681_Italy
Panaeolus_cinctulus_Gerhardt83052_1_Germany
ET
Panaeolus cinctulus
1/87
-/93
Panaeolus_charrua_MVHC5775_Uruguay
Panaeolus_charrua_MVHC5833_Uruguay
Panaeolus_charrua_MVHC5825_Uruguay
Panaeolus_charrua_MVHC5835_Uruguay
T
Panaeolus charrua
1/98
Panaeolus_foenisecii_TUF117010_Canada
Panaeolus_foenisecii_TUF118243_Estonia
Panaeolus_foenisecii_KM250281_United_Kingdom
Panaeolus_foenisecii_MCVE6643_Italy
Panaeolus_foenisecii_iNat118906067_USA
Panaeolus_foenisecii_iNAT21657597_USA
Panaeolus_foenisecii_MycoMap5431_USA
Panaeolus_foenisecii_OTA71571_New_Zealand
Panaeolus_foenisecii_M8_Hungary
Panaeolus_foenisecii_ubcF32593_Canada
Panaeolus_foenisecii_MycoMap5509_USA
Panaeolus_foenisecii_TUF105754_Denmark
Panaeolus_foenisecii_Z39_USA
Panaeolus_foenisecii_AMB20072_Italy
Panaeolus_foenisecii_AMB20071_Italy
Panaeolus_foenisecii_CBS142_40_Unknown
Panaeolus_papilionaceus_CIRM_BRFM715_Unknown
Panaeolus_foenisecii_MVHC5862_Uruguay
Panaeolus foenisecii
0.99/87
0.72/96
1/99
0.02
A

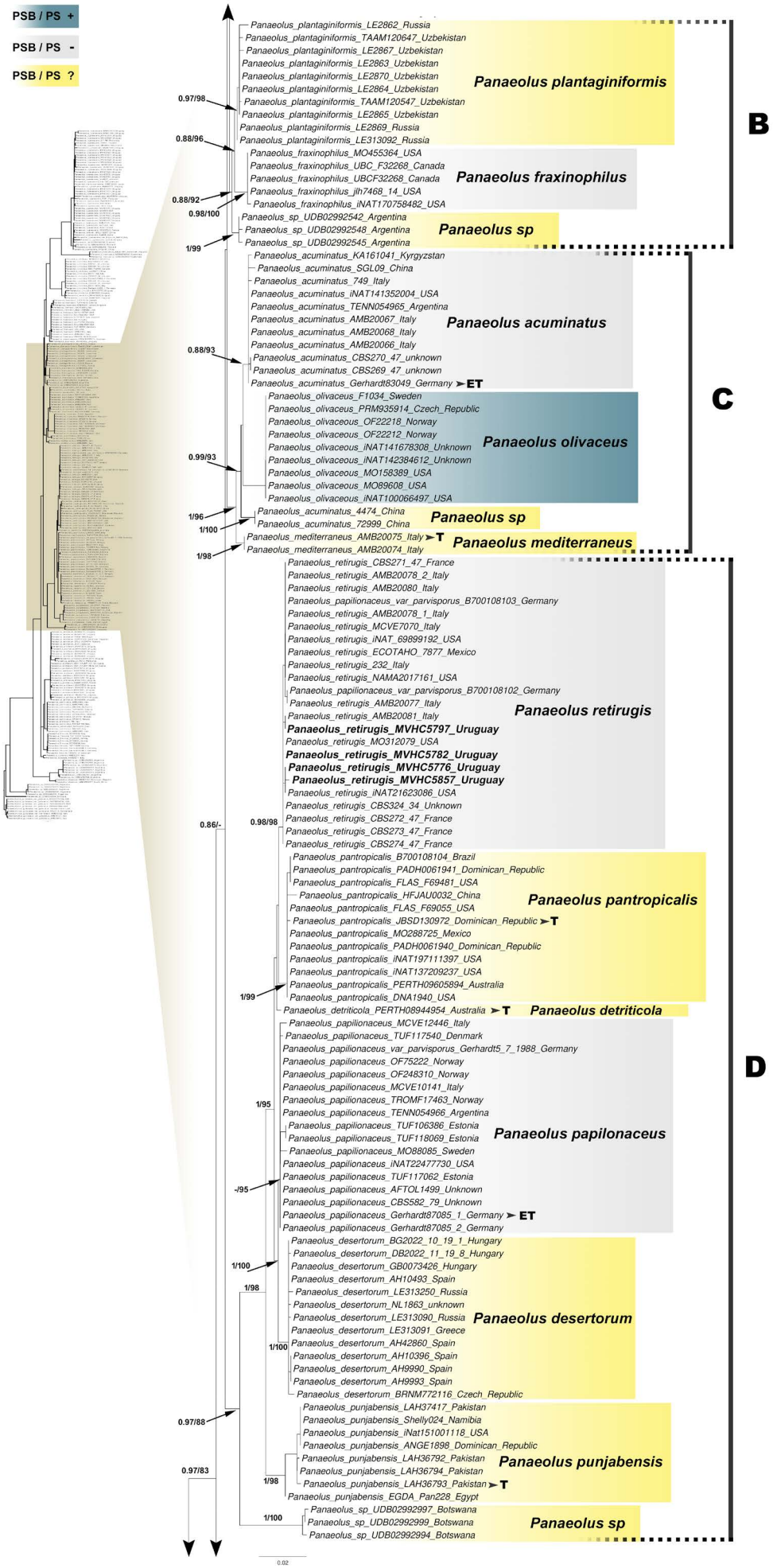
PSB / PS +
PSB / PS -
PSB / PS ?
Panaeolus_plantaginiformis_LE2862_Russia
Panaeolus_plantaginiformis_TAAM120647_Uzbekistan
Panaeolus_plantaginiformis_LE2867_Uzbekistan
Panaeolus_plantaginiformis_LE2863_Uzbekistan
Panaeolus_plantaginiformis_LE2870_Uzbekistan
Panaeolus_plantaginiformis_LE2864_Uzbekistan
Panaeolus_plantaginiformis_TAAM120547_Uzbekistan
Panaeolus_plantaginiformis_LE2865_Uzbekistan
Panaeolus_plantaginiformis_LE2869_Russia
Panaeolus_plantaginiformis_LE313092_Russia
Panaeolus plantaginiformis
0.97/98
0.88/96
Panaeolus_fraxinophilus_MO455364_USA
Panaeolus_fraxinophilus_UBC_F32268_Canada
Panaeolus_fraxinophilus_UBCF32268_Canada
Panaeolus_fraxinophilus_jlh7468_14_USA
Panaeolus_fraxinophilus_iNAT170758482_USA
Panaeolus fraxinophilus
0.88/92
0.98/100
Panaeolus_sp_UDB02992542_Argentina
Panaeolus_sp_UDB02992548_Argentina
Panaeolus_sp_UDB02992545_Argentina
Panaeolus sp
1/99
B
Panaeolus_acuminatus_KA161041_Kyrgyzstan
Panaeolus_acuminatus_SGL09_China
Panaeolus_acuminatus_749_Italy
Panaeolus_acuminatus_iNAT141352004_USA
Panaeolus_acuminatus_TENN054965_Argentina
Panaeolus_acuminatus_AMB20067_Italy
Panaeolus_acuminatus_AMB20068_Italy
Panaeolus_acuminatus_AMB20066_Italy
Panaeolus acuminatus
0.88/93
Panaeolus_acuminatus_CBS270_47_unknown
Panaeolus_acuminatus_CBS269_47_unknown
Panaeolus_acuminatus_Gerhardt83049_Germany ➤ET
Panaeolus_olivaceus_F1034_Sweden
Panaeolus_olivaceus_PRM935914_Czech_Republic
Panaeolus_olivaceous_OF22218_Norway
Panaeolus_olivaceous_OF22212_Norway
Panaeolus_olivaceous_iNAT141678308_Unknown
Panaeolus_olivaceous_iNAT142384612_Unknown
Panaeolus_olivaceous_MO158389_USA
Panaeolus_olivaceous_MO89608_USA
Panaeolus_olivaceous_iNAT100066497_USA
Panaeolus olivaceus
0.99/93
C
1/96
1/100
Panaeolus_acuminatus_4474_China
Panaeolus_acuminatus_72999_China
Panaeolus sp
Panaeolus_mediterraneus_AMB20075_Italy ➤T
Panaeolus_mediterraneus_AMB20074_Italy
Panaeolus mediterraneus
1/98
Panaeolus_retirugis_CBS271_47_France
Panaeolus_retirugis_AMB20078_2_Italy
Panaeolus_retirugis_AMB20080_Italy
Panaeolus_papilionaceus_var_parvisporus_B700108103_Germany
Panaeolus_retirugis_AMB20078_1_Italy
Panaeolus_retirugis_MCVE7070_Italy
Panaeolus_retirugis_iNAT_69899192_USA
Panaeolus_retirugis_ECOTAHO_7877_Mexico
Panaeolus_retirugis_232_Italy
Panaeolus_retirugis_NAMA2017161_USA
Panaeolus_papilionaceus_var_parvisporus_B700108102_Germany
Panaeolus_retirugis_AMB20077_Italy
Panaeolus_retirugis_AMB20081_Italy
Panaeolus retirugis
Panaeolus_retirugis_MVHC5797_Uruguay
Panaeolus_retirugis_MO312079_USA
Panaeolus_retirugis_MVHC5782_Uruguay
Panaeolus_retirugis_MVHC5776_Uruguay
Panaeolus_retirugis_MVHC5857_Uruguay
Panaeolus_retirugis_iNAT21623086_USA
Panaeolus_retirugis_CBS324_34_Unknown
Panaeolus_retirugis_CBS272_47_France
Panaeolus_retirugis_CBS273_47_France
Panaeolus_retirugis_CBS274_47_France
0.86/-
0.98/98
Panaeolus_pantropicalis_B700108104_Brazil
Panaeolus_pantropicalis_PADH0061941_Dominican_Republic
Panaeolus_pantropicalis_FLAS_F69481_USA
Panaeolus_pantropicalis_HFJAU0032_China
Panaeolus_pantropicalis_FLAS_F69055_USA
Panaeolus_pantropicalis_JBSD130972_Dominican_Republic ➤T
Panaeolus_pantropicalis_MO288725_Mexico
Panaeolus_pantropicalis_PADH0061940_Dominican_Republic
Panaeolus_pantropicalis_iNAT197111397_USA
Panaeolus_pantropicalis_iNAT137209237_USA
Panaeolus_pantropicalis_PERTH09605894_Australia
Panaeolus_pantropicalis_DNA1940_USA
Panaeolus pantropicalis
1/99
Panaeolus_detriticola_PERTH08944954_Australia ➤T
Panaeolus detriticola
Panaeolus_papilionaceus_MCVE12446_Italy
Panaeolus_papilionaceus_TUF117540_Denmark
Panaeolus_papilionaceus_var_parvisporus_Gerhardt5_7_1988_Germany
Panaeolus_papilionaceus_OF75222_Norway
Panaeolus_papilionaceus_OF248310_Norway
Panaeolus_papilionaceus_MCVE10141_Italy
Panaeolus_papilionaceus_TROMF17463_Norway
Panaeolus_papilionaceus_TENN054966_Argentina
1/95
Panaeolus_papilionaceus_TUF106386_Estonia
Panaeolus_papilionaceus_TUF118069_Estonia
Panaeolus_papilionaceus_MO88085_Sweden
Panaeolus_papilionaceus_iNAT22477730_USA
Panaeolus_papilionaceus_TUF117062_Estonia
Panaeolus_papilionaceus_AFTOL1499_Unknown
Panaeolus_papilionaceus_CBS582_79_Unknown
Panaeolus_papilionaceus_Gerhardt87085_1_Germany ➤ ET
Panaeolus_papilionaceus_Gerhardt87085_2_Germany
Panaeolus papilonaceus
-/95
D
Panaeolus_desertorum_BG2022_10_19_1_Hungary
Panaeolus_desertorum_DB2022_11_19_8_Hungary
Panaeolus_desertorum_GB0073426_Hungary
Panaeolus_desertorum_AH10493_Spain
Panaeolus_desertorum_LE313250_Russia
Panaeolus_desertorum_NL1863_unknown
Panaeolus_desertorum_LE313090_Russia
Panaeolus_desertorum_LE313091_Greece
Panaeolus_desertorum_AH42860_Spain
Panaeolus_desertorum_AH10396_Spain
Panaeolus_desertorum_AH9990_Spain
Panaeolus_desertorum_AH9993_Spain
Panaeolus_desertorum_BRNM772116_Czech_Republic
Panaeolus desertorum
1/100
1/98
1/100
Panaeolus_punjabensis_LAH37417_Pakistan
Panaeolus_punjabensis_Shelly024_Namibia
Panaeolus_punjabensis_iNat151001118_USA
Panaeolus_punjabensis_ANGE1898_Dominican_Republic
Panaeolus_punjabensis_LAH36792_Pakistan
Panaeolus_punjabensis_LAH36794_Pakistan
Panaeolus_punjabensis_LAH36793_Pakistan ➤T
Panaeolus_punjabensis_EGDA_Pan228_Egypt
Panaeolus punjabensis
0.97/88
0.97/83
1/98
Panaeolus_sp_UDB02992997_Botswana
Panaeolus_sp_UDB02992999_Botswana
Panaeolus_sp_UDB02992994_Botswana
Panaeolus sp
1/100
0.02

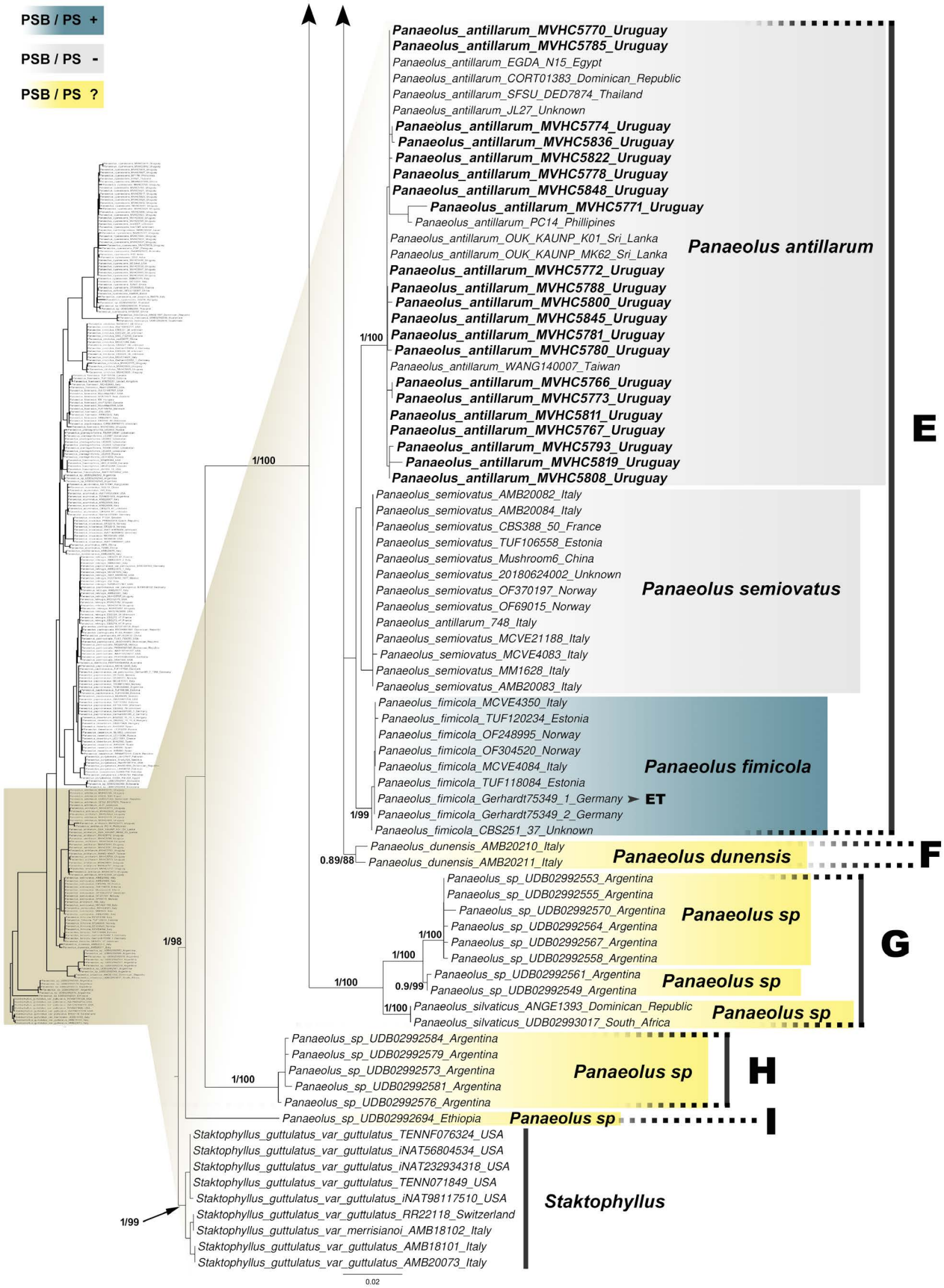

Fig. 1. Maximum Likelihood tree of *Panaeolus* based on concatenated dataset of ITS + LSU sequence data. Branch support values are shown as BPP/BS, ≥ 0.7 and ≥ 70 respectively. Specimens sequenced in this work are highlighted in bold. For each species, the content of psychoactive alkaloids PSB/PS: presence (+), absence (-), unknown (?) is indicated with blue, gray and yellow respectively, based on chemical analyses performed in this work and literature records (Guzmán & Petrarca 1972, Young 1989, Guzman et al. 1998, Senn-Irlet et al. 1999, Allen 2010, Voto & Angelini 2021, Gotvaldová et al. 2022, Strauss et al. 2023 and the references within). T= type specimen, ET= epitype specimen.

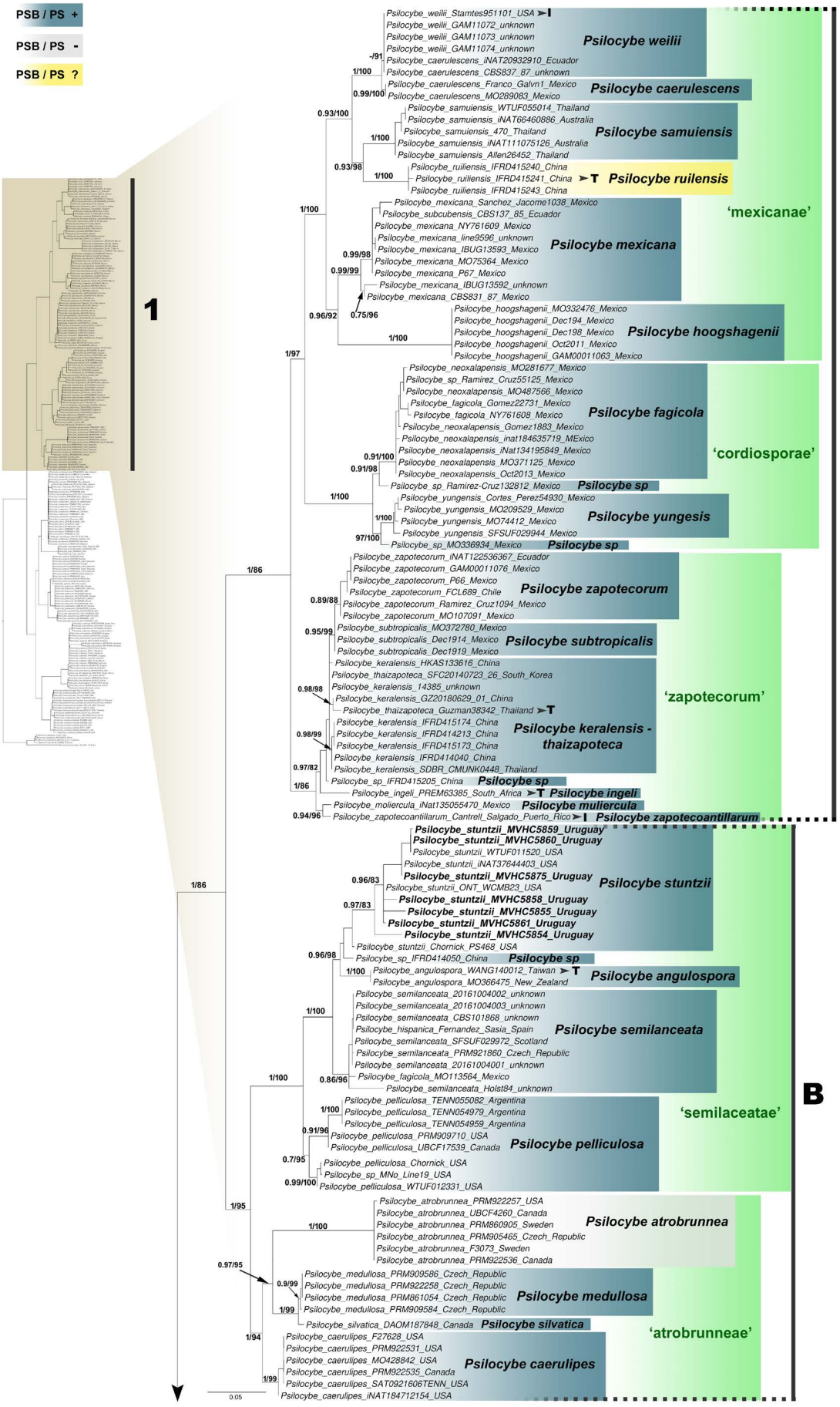
PSB / PS +
PSB / PS -
PSB / PS ?
1
A
B
Psilocybe weilii_Stamtes951101_USA ➤I
Psilocybe_weilii_GAM11072_unknown
Psilocybe_weilii_GAM11073_unknown
Psilocybe_weilii_GAM11074_unknown
Psilocybe weilii
Psilocybe_caerulescens_iNAT20932910_Ecuador
Psilocybe_caerulescens_CBS837_87_unknown
Psilocybe_caerulescens_Franco_Galvn1_Mexico
Psilocybe_caerulescens_MO289083_Mexico
Psilocybe caerulescens
Psilocybe_samuiensis_WTUF055014_Thailand
Psilocybe_samuiensis_iNAT664460886_Australia
Psilocybe_samuiensis_470_Thailand
Psilocybe_samuiensis_iNAT111075126_Australia
Psilocybe_samuiensis_Allen26452_Thailand
Psilocybe samuiensis
Psilocybe_ruiliensis_IFRD415240_China
Psilocybe_ruiliensis_IFRD415241_China ➤T
Psilocybe_ruiliensis_IFRD415243_China
Psilocybe ruilensis
'mexicanae'
Psilocybe_mexicana_Sanchez_Jacome1038_Mexico
Psilocybe_subcubensis_CBS137_85_Ecuador
Psilocybe_mexicana_NY761609_Mexico
Psilocybe_mexicana_line9596_unknown
Psilocybe_mexicana_IBUG13593_Mexico
Psilocybe mexicana
Psilocybe_mexicana_MO75364_Mexico
Psilocybe_mexicana_P67_Mexico
Psilocybe_mexicana_IBUG13592_unknown
Psilocybe_mexicana_CBS831_87_Mexico
Psilocybe_hoogshagenii_MO332476_Mexico
Psilocybe_hoogshagenii_Dec194_Mexico
Psilocybe_hoogshagenii_Dec198_Mexico
Psilocybe hoogshagenii
Psilocybe_hoogshagenii_Oct2011_Mexico
Psilocybe_hoogshagenii_GAM00011063_Mexico
Psilocybe_neoxalapensis_MO281677_Mexico
Psilocybe_sp_Ramirez_Cruz55125_Mexico
Psilocybe_neoxalapensis_MO487566_Mexico
Psilocybe_fagicola_Gomez22731_Mexico
Psilocybe_fagicola_NY761608_Mexico
Psilocybe fagicola
'cordiosporae'
Psilocybe_neoxalapensis_Gomez1883_Mexico
Psilocybe_neoxalapensis_inat184635719_MExico
Psilocybe_neoxalapensis_iNat134195849_Mexico
Psilocybe_neoxalapensis_MO371125_Mexico
Psilocybe_neoxalapensis_Oct2013_Mexico
Psilocybe_sp_Ramirez-Cruz132812_Mexico
Psilocybe sp
Psilocybe_yungensis_Cortes_Perez54930_Mexico
Psilocybe_yungensis_MO209529_Mexico
Psilocybe_yungensis_MO74412_Mexico
Psilocybe yungesis
Psilocybe_yungensis_SFSUF029944_Mexico
Psilocybe_sp_MO336934_Mexico
Psilocybe sp
Psilocybe_zapotecorum_iNAT122536367_Ecuador
Psilocybe_zapotecorum_GAM00011076_Mexico
Psilocybe_zapotecorum_P66_Mexico
Psilocybe_zapotecorum_FCL689_Chile
Psilocybe zapotecorum
Psilocybe_zapotecorum_Ramirez_Cruz1094_Mexico
Psilocybe_zapotecorum_MO107091_Mexico
Psilocybe_subtropicalis_MO372780_Mexico
Psilocybe_subtropicalis_Dec1914_Mexico
Psilocybe_subtropicalis_Dec1919_Mexico
Psilocybe subtropicalis
Psilocybe_keralensis_HKAS133616_China
Psilocybe_thaizapoteca_SFC20140723_26_South_Korea
Psilocybe_keralensis_14385_unknown
Psilocybe_keralensis_GZ20180629_01_China
Psilocybe_thaizapoteca_Guzman38342_Thailand ➤T
'zapotecorum'
Psilocybe_keralensis_IFRD415174_China
Psilocybe_keralensis_IFRD414213_China
Psilocybe_keralensis_IFRD415173_China
Psilocybe keralensis - thaizapoteca
Psilocybe_keralensis_IFRD414040_China
Psilocybe_keralensis_SDBR_CMUNK0448_Thailand
Psilocybe_sp_IFRD415205_China
Psilocybe sp
Psilocybe_ingeli_PREM63385_South_Africa ➤T
Psilocybe ingeli
Psilocybe_moliercula_iNat135055470_Mexico
Psilocybe muliercula
Psilocybe_zapotecoantillarum_Cantrell_Salgado_Puerto_Rico ➤I
Psilocybe zapotecoantillarum
Psilocybe_stuntzii_MVHC5859_Uruguay
Psilocybe_stuntzii_MVHC5860_Uruguay
Psilocybe_stuntzii_WTUF011520_USA
Psilocybe_stuntzii_iNAT37644403_USA
Psilocybe_stuntzii_MVHC5875_Uruguay
Psilocybe stuntzii
Psilocybe_stuntzii_ONT_WCMB23_USA
Psilocybe_stuntzii_MVHC5858_Uruguay
Psilocybe_stuntzii_MVHC5855_Uruguay
Psilocybe_stuntzii_MVHC5861_Uruguay
Psilocybe_stuntzii_MVHC5854_Uruguay
Psilocybe_stuntzii_Chornick_PS468_USA
Psilocybe_sp_IFRD414050_China
Psilocybe sp
Psilocybe_angulospora_WANG140012_Taiwan ➤T
Psilocybe_angulospora_MO366475_New_Zealand
Psilocybe angulospora
Psilocybe_semilanceata_20161004002_unknown
Psilocybe_semilanceata_20161004003_unknown
Psilocybe_semilanceata_CBS101868_unknown
Psilocybe_hispanica_Fernandez_Sasia_Spain
Psilocybe semilanceata
Psilocybe_semilanceata_SFSUF029972_Scotland
Psilocybe_semilanceata_PRM921860_Czech_Republic
Psilocybe_semilanceata_20161004001_unknown
Psilocybe_fagicola_MO113564_Mexico
Psilocybe_semilanceata_Holst84_unknown
'semilaceatae'
Psilocybe_pelliculosa_TENN055082_Argentina
Psilocybe_pelliculosa_TENN054979_Argentina
Psilocybe_pelliculosa_TENN054959_Argentina
Psilocybe_pelliculosa_PRM909710_USA
Psilocybe_pelliculosa_UBCF17539_Canada
Psilocybe pelliculosa
Psilocybe_pelliculosa_Chornick_USA
Psilocybe_sp_MNo_Line19_USA
Psilocybe_pelliculosa_WTUF012331_USA
Psilocybe_atrobrunnea_PRM922257_USA
Psilocybe_atrobrunnea_UBCF4260_Canada
Psilocybe_atrobrunnea_PRM860905_Sweden
Psilocybe_atrobrunnea_PRM905465_Czech_Republic
Psilocybe atrobrunnea
Psilocybe_atrobrunnea_F3073_Sweden
Psilocybe_atrobrunnea_PRM922536_Canada
Psilocybe_medullosa_PRM909586_Czech_Republic
Psilocybe_medullosa_PRM922258_Czech_Republic
Psilocybe_medullosa_PRM861054_Czech_Republic
Psilocybe medullosa
Psilocybe_medullosa_PRM909584_Czech_Republic
Psilocybe_silvatica_DAOM187848_Canada
Psilocybe silvatica
'atrobrunneae'
Psilocybe_caerulipes_F27628_USA
Psilocybe_caerulipes_PRM922531_USA
Psilocybe_caerulipes_MO428842_USA
Psilocybe_caerulipes_PRM922535_Canada
Psilocybe caerulipes
Psilocybe_caerulipes_SAT0921606TENN_USA
Psilocybe_caerulipes_iNAT184712154_USA
0.05

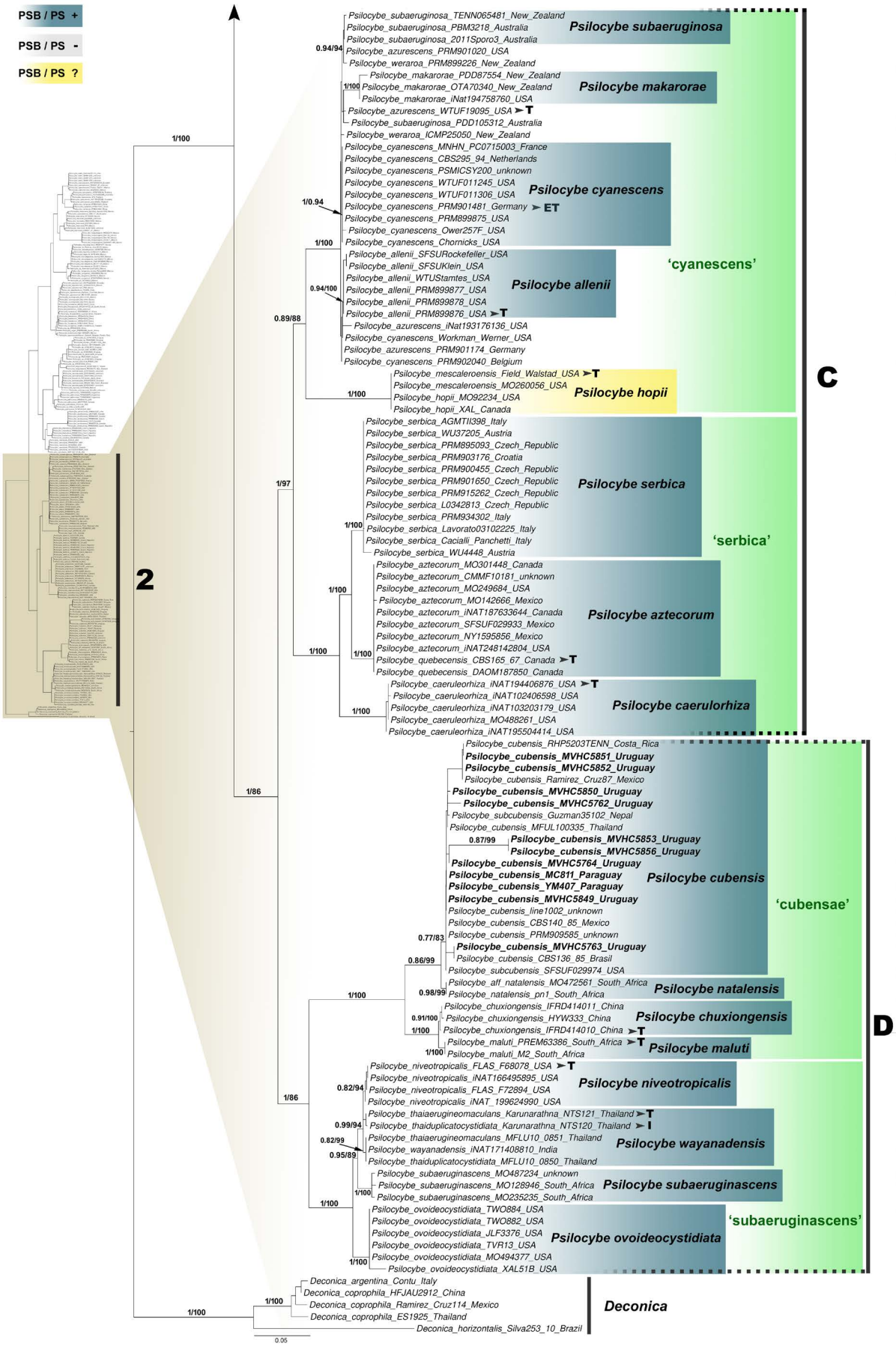

Fig. 2. Maximum Likelihood tree of *Psilocybe* based on concatenated dataset of ITS + LSU + *rpb2* + *tef1* sequence data. Branch support values are shown as BPP/BS, Bayesian posterior probability above 0.7 and Bootstrap values above 70 %. Specimens sequenced in this work are highlighted in bold. For each species, the content of psychoactive alkaloids PSB/PS: presence (+), absence (-), unknown (?) is indicated with blue, gray and yellow respectively, based on chemical analyses performed in this work and literature records [Høiland 1978, Allen 2010 (and the references within), Borovicka *et al*. 2012, Guzman *et al*. 2012, Hyde 2014, Borovicka *et al*. 2015, Wang & Tzean 2015, Li *et al.* 2020, Nkadimeng *et al.* 2020, Allen *et al.* 2024, Canan *et al.* 2024, Ostuni *et al.* 2024]. T = type specimen, I = isotype specimen.

Taxonomy

Based on morphological and phylogenetic analyses, five species of *Paneolus* were identified, one of them new to science, along with two species of *Psilocybe*. Detailed morphological descriptions based on the studied specimens are presented below. For each species, a taxonomic discussion and the results of alkaloid content analysis are included.

Panaeolus antillarum (Fr.) Dennis, *Kew Bull*. **15**(1): 124. 1961. Fig. 3A–M.

Description: *Pileus* 0.8–10 × 0.7–5 cm, conical to convex or broadly parabolic, occasionally hemispherical to conico-campanulate; surface shiny, dry, non-hygrophanous, and glabrous, becoming wrinkled, lacunose, or irregularly rimose at maturity. Color varying with gray valleys (5B1; Gray) and yellowish-brown ridges (5E5; Yellowish Brown) or creamy-whitish tones (5E3; Pale Orange). When dry, the pileus appears homogeneous, rough, beige (5E7; Yellowish Brown), and shiny, sometimes exhibiting a grayish sheen (5D1; Gray). *Margin* straight to slightly incurved, entire, finely undulating to eroded when dry, concolorous with the pileus surface. *Lamellae* adnate to adnexed, close to crowded; edge entire, smooth, whitish to dark when dry; faces waxy, dark grayish (5F1; Gray) to black, mottled. *Stipe* 2–15 × 0.2–1.2 cm, central, cylindrical. Surface slightly pruinose to longitudinally striate (from apex to base), fibrous, hard, and brittle. Color whitish to yellowish-brown, consistent with the pileus surface. *Context* 0.1–0.2 cm thick, fleshy, whitish. *Veil* absent. *Spore print* blackish. *Basidiospores* (10.3–)14.5–20(–21.8) × (7.3–)8.9–12.9(–13.9) × (–5.8)6.7–10.9(–12.8) µm, Q = 1.49–1.69, Q_m = 1.69, limoniform to subhexagonal in frontal view and ellipsoid in lateral view, dark brown to blackish, smooth, thick walls 1.2–1.5 µm thick and a truncated germ pore 1.1–2.5 µm. *Basidia* 16.2–32.5 × 6.4–17.5 µm, irregularly cushion-shaped to pyriform, hyaline, tetrasporic. *Pleurocystidia* 20–56.5 × 10.1–25.8 µm, chrysocystidia, sulphidia type, hyaline, thin-walled, clavate to occasionally cylindrical, some mucronate or papillate, with refractive and irregular greenish-grayish content in KOH. *Cheilocystidia* 13.8–41.9 × 4.3–20 µm, sparse, grouped, polymorphic, cylindrical, short-clavate, fusiform, with broad and obtuse apex or lageniform, hyaline, and thin-walled. *Hymenophoral trama* composed of smooth, hyaline, thin-walled hyphae, cylindrical (up to 4.3 µm) or more commonly inflated (5.6–11.7 µm). *Pileipellis* formed by an epithelium of isodiametric to pyriform cells, smooth, thin-walled, 12.2–44.6 µm diam. *Pileal trama* composed of interwoven, thin-walled hyphae, 3.3–5.1 µm diam. *Stipitipellis* a cutis of interwoven hyaline, thin-walled hyphae, 4.9–7.9 µm diam. *Caulocystidia* 19–69.6 × 3.5–14.7 µm, leptocystidia, cylindrical, hyaline, thin-walled, with an obtuse apex.

Specimens examined: **Uruguay**, Montevideo, Manga, S34°48’26”, W56°08’17, 37 m.a.s.l., peri-urban field, on cow dung, 1 Apr. 2021, *G. Morera* (MVHC 5748, MVHC 5766 and MVHC 5767); Colonia, S33°58’23.4”, W57°16’56.7”, 20 m.a.s.l., open meadow with cattle, on horse dung, 8 Feb. 2022, *G. Morera et al.* (MVHC 5770-74, MVHC 5778-80 MVHC 5781, MVHC 5783-96, MVHC 5798-5815); Maldonado, Sierra de las Ánimas, S34°36’, W55°17’, 209 m.a.s.l., on cow dung, 3 Mar. 2022, *G. Morera* & *S. Lupo* (MVHC 5819, MVHC 5822, MVHC 5836 and MVHC 5845); Tacuarembó, S31°42’40”S, W55°58’44”, 137 m.a.s.l., on cow dung, May 2022, *S. Lupo* (MVHC 5848).

Habit, habitat and distribution: Cosmopolitan in tropical to subtropical regions (Voto and Angelini 2024, Strauss *et al.* 2023). It was firstly registered in Uruguay by Gerhardt (1996) and recently recorded by Sequeira (2017). Found growing solitary or in groups up to 4 specimens, in horse and cow dung.

Notes: *Panaeolus antillarum* is a coprophilous cosmopolitan species originally described from the Antilles, Dominican Republic (Fries 1828, Dennis 1961), where it was found growing on mule dung. However, it has also been observed on cow, horse, and even elephant dung, among other substrates (De & Perry 2017). It is characterized by basidiomata of medium size, with the pileus convex or broadly parabolic, reaching up to 10 cm diam., with a pale grayish or whitish coloration and lacking annulus. Microscopically, the species is distinguishable by its large basidiospores (up to 21.8 µm in length, subhexagonal in frontal view) and pleurocystidia that are mucronate or papillate, containing refractive and irregular greenish gray content in KOH. These characteristics align with the observations of Guzman & Petrarca (1972), Gerhardt (1996), Kaur *et al*. (2014) and Voto & Angelini (2024). Phylogenetically, *Pa. antillarum* is closely related to *Pa. semiovatus* and *Pa. fimicola* (Fig. 1), two pale-colored species that also possess sulphidia-type chrysocystidia (Hesler 2013, Consiglio & Marchetti 2025). *Panaeolus antillarum* can be distinguished from *Pa. semiovatus* by the absence of an annulus or any remnants of a marginal veil on the pileus (Voto & Angelini 2024), and from *Pa. fimicola*, which produces markedly smaller basidiospores reaching about 12 µm (Consiglio & Marchetti 2025). *Panaeolus antillarum* was initially classified as a hallucinogenic species (Guzmán 1959); however, recent studies have provided evidence for the absence of psychoactive indole alkaloids such as psilocybin, psilocin, or baeocystin in this species (Young 1989, Allen 2010, Strauss *et al*. 2023, this work). This misconception could have been due to confusion with other potentially hallucinogenic species, such as *Pa. fimicola* or *Pa. cyanescens*.

Panaeolus charrua Morera, Lupo, Martínez Kopp & Robledo, ***sp. nov.*** Fig 4A–J. MB 862528.

Etymology: Named after the Charrúa people, Indigenous inhabitants of Uruguay and neighboring regions of southern South America.

Typus: **Uruguay**, Maldonado, Sierra de las Ánimas, S34°36’, W55°17’ elev. 209 m.a.s.l., on cow dung, 3 Mar. 2022, *G. Morera* & *S. Lupo* (**holotype** MVHC 5835).

Description: *Pileus* 0.5–2.5 × 1–2 cm (generally twice as high as wide), mostly secotioid, occasionally conical-umbonate, parabolic, or campanulate; surface opaque, dry, non-hygrophanous, glabrous, smooth to wrinkled, yellowish or light brown (5D6; Yellowish Brown), with concentric

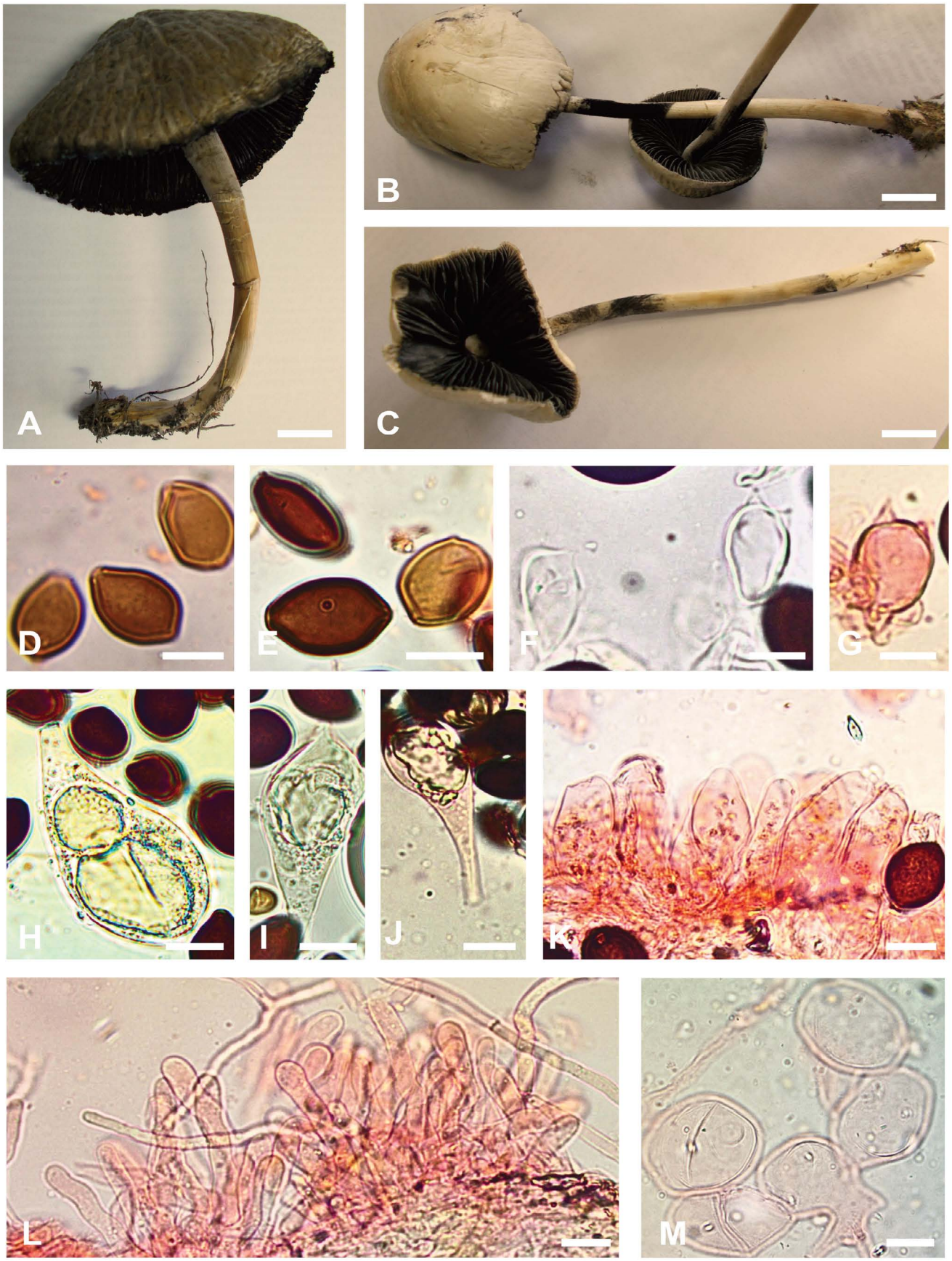

Fig. 3. *Panaeolus antillarum*. Basidomata. **A.** MVHC 5770. **B, C.** MVHC 5774. Basidiospores. **D, E.** MVHC 5770. Basidia. **F.** MVHC 5770. **G.** MVHC 5780. Pleurocystidia. **H, I.** MVHC 5774. **J.** MVHC 5791. Cheilocystidia. **K.** MVHC 5783. Caulocystidia. **L.** MVHC 5795. Pileocystida. **M.** MVHC 5780. Scale bars: A–C= 1 cm, D–M = 10 µm.

Fig. 4. *Panaeolus charrua*. Basidomata. **A, B.** MVHC 5826. Basidiospores. **C.** MVHC 5835. Basidia. **D.** MVHC 5775. **E, F.** MVHC 5826. Cheilocystidia. **G**. MVHC 5835. Caulocystidia. **H.** MVHC 5826. Pileocystida. **I, J.** MVHC 5775. Scale bars: A, B = 1 cm, C–J = 10 µm.

striations and tears when fresh. *Margin* irregular, straight, sometimes incurved or nearly attached to the stipe, entire, then eroded, initially concolorous, later darkened (5F4; Olive Brown). *Lamellae* adnate or adnexed, close to crowded, waxy, whitish when fresh (7A2; Pinkish White), dark grayish (5F1; Gray) when mature, not mottled. Edge thick, entire, light brown when fresh, turning grayish. Stipe 6–10 × 0.1–0.4 cm, cylindrical, striated (longitudinally helicoidal), glabrous, hollow, fibrous, and fistulose. Inner surface dark, outer surface concolorous with the pileus, with darker longitudinal bruises. *Context* 0.1–0.2 cm, fibrous to corky, whitish to light brown (4A2; Yellowish White). *Veil* absent. *Spore print* dark gray to graphite colored. *Basidiospores* (10–)11.6–15.6(–16) × (6.9–)7.2–10.1(–10.5) × (3.8–)5.3–8(–8.6) µm, Q= 1.5–1.87, Q_m= 1.85, ovoid to rhomboid in frontal view, and ellipsoidal in lateral view, with a slightly flattened side. Color light to dark brown, with walls up to 1.3 µm thick, smooth, with a conspicuous truncate germ pore, up to 1.8 µm. *Basidia* 12.4–38.9 × 6–15.1 µm, clavate to sub-spherical, with 1–4 sterigmata, normal to thickened, sometimes very

long (up to 53 µm), other times branching from a central axis (up to 24 µm). *Pseudoparaphyses* often observed, generally utriform to ovoid, 16.4 × 10 µm in average. *Pleurocystidia* not seen. *Cheilocystidia* 16.4–40.8 × 4.8–14.2 µm, hyaline, thin-walled, lageniform, sometimes ventricose, rarely cylindrical. *Hymenophoral trama* composed of smooth, irregularly arranged hyphae, filamentous or more commonly inflated up to 12 µm. *Pileipellis* composed of an epithelium of spherical pedunculated cells, 18.4–51.9 × 10.6–33.5 µm. *Pileocystidia* hyaline, thin-walled, clavate, 17.4–52.5 × 4.7–20.2 µm. *Stipitipellis* a cutis of longitudinally arranged, yellowish brown hyphae, up to 8 µm wide. *Caulocystidia* 17.1–45.1 × 2.4–12.6 µm, polymorphic, cylindrical, clavate, sometimes ventricose, with a conspicuous wall in the apice.

Other collections examined: **Uruguay**, Colonia, S33°58'23.4", W57°16'56.7", 20 m.a.s.l., open meadow with cattle, on horse dung, 8 Feb. 2022, *G. Morera et al.* (MVHC 5775); Maldonado, Sierra de las Ánimas, S34°36'S, W55°17', 209 m.a.s.l., on cow dung, 3 Mar. 2022, *G. Morera* & *S. Lupo* (MVHC 5825, MVHC 5826 and MVHC 5833).

Habit, habitat and distribution: So far, it is only known from Uruguay, where it grows gregariously on cow dung, forming groups of up to 20 specimens.

Notes: *Panaeolus charrua* represents a new species characterized by a mostly enclosed pileus that is approximately twice as tall as it is wide, and by whitish to dark grayish, non-mottled lamellae. It presents a long (6–10 cm), longitudinally helicoid-striate stipe. Microscopically, it forms basidia with irregular sterigmata in shape (sometimes branched), length (up to 53 µm), and number (1–4). The general morphology of this new species, the combination of gasteroid and agaricoid basidiomata with *Panaeolus* micromorphology, resembles partially that of species traditionally known as *Galeropsis* (Velenovský 1930) and *Panaeolopsis* (Singer 1969). Historically the species classified in *Galeropsis* were later transferred from one to other genera (e.g., *Galera*, *Bolbitius*, *Conocybe*, *Agrocybe*, *Gastrocybe*, *Secotium*, *Weraroa*, *Cyttarophyllum*, *Psammomyces*), illustrating the taxonomic complexity and circumscription difficulties associated with this group. Since the 2000s, DNA-based studies have revealed the polyphyletic nature of *Galeropsis* (Tóth *et al*. 2013, Malysheva *et al*. 2019). On the other hand, *Panaeolopsis*, considered the secotioid counterpart of *Panaeolus*, is now considered an artificial genus and was recently synonymized with *Panaeolus* (Angelini & Voto 2023). *Panaeolus desertorum* and *Pa. plantaginiformis* are two species previously considered in *Galeropsis* (Malysheva *et al.* 2019). *Panaeolus charrua* differs from *Pa. desertorum* in its obtuse (not acute) pileus apex, smaller basidiospores (10–16 × 6.9–10.5 × 3.8–8 µm vs 12.5–21.7 × 6.3–17.7 µm), and longer sterigmata (53 µm vs 20 µm). Moreover, *Pa. desertorum* lacks cheilocystidia and has a Eurasian distribution (Malysheva *et al.* 2019). The general macromorphology of the type of *Pa. charrua* is reminiscent of *Pa. plantaginiformis*, however, the color of the lamellae in *Pa. plantaginiformis* is ochraceous brown in contrast with the dark grayish of *Pa. charrua*. Microscopically, both species are very similar (including basidiospore and basidia size, as well as cheilocystidia morphology), but differ by the absence of caulocystidia in *Pa. plantaginiformis*. Although *Pa. plantaginiformis* has been reported to have a worldwide distribution and has been reported from Argentina (Malysheva *et al.* 2019), it is phylogenetically unrelated to *Pa. charrua* and so far only known from Russia and Uzbekistan (Fig. 1). For their part, there are 4 ex-*Panaeolopsis* species close to *Pa. charrua*: *Pa. brasiliensis*, *Pa. nirimbii*, *Pa. obtusus*, and *Pa. sanmartinianus*. *Panaeolus brasiliensis* features a stipe with a bulbous base and subglobose basidiospores, unlike what is observed in *Pa. charrua* (Singer 1976). *Panaeolus sanmartinianus*, described from Argentina, differs from *Pa. charrua* by its ring-like basal opening of the mature pileus, smoky-black fusiform basidiospores, and the presence of pileocystidia similar to cheilocystidia (Singer 1969). The macromorphology of *Pa. nirimbii* also resembles that of *Pa. charrua*, however, *P. nirimbii* was described from Australia, growing on soil, and lacks descriptions of aberrant basidia, pseudoparaphyses (Young 1989), or a longitudinally helicoid-striate stipe (Voto & Angelini 2024). *Panaeolus obtusus* is a similar species with smaller basidia (up to 20 µm) that was described from Italy in soil with herbaceous plants (Contu 1998), unlike our specimens, which always grow from dung and show larger basidia (up to 38.9 µm). Moreover, the description by Contu (1998) does not provide details of the pileipellis nor comments on the presence of paraphyses (Contu 1998, Angelini & Voto 2023). Considering its unique morphological, ecological, geographical, and phylogenetic traits, we propose *Pa. charrua* as a new species. Regarding the alkaloid content, no detectable amounts of PSB and PS were observed (Table 1).

Panaeolus cyanescens Sacc., *Syll. Fung*. (Abellini) **5**: 1123. 1887. Fig. 5A–L.

Description: *Pileus* 0.5–4.5 × 0.5–1.8 cm, conical, campanulate-conical, or broadly parabolic, later becoming convex and eventually appearing flat; when dry, may exhibit an umbo; surface variable in luster, glabrous, dry to slightly subviscid, non-hygrophanous, and tending to become cerulescent upon handling, rimose at maturity. Color initially very pale brown to solid creamy white (3A2; yellowish white), sometimes with fine radial ornamentation, later becoming woody brown (5D5; light brown) with irregular deep cracks (except at the center). *Margin* straight or incurved, initially entire, later irregular and eroded, becoming dark and deeply rimose like the surface, concolorous with the surface or lighter, and cerulescent. *Lamellae* adnate to adnexed, close to crowded, pruinose, gray (5E6; gray) to ashy mottled, becoming blackish at maturity, with edges concolorous to the face or whitish (dark at maturity), entire to slightly serrated in exceptional cases. *Stipe* 2–8 cm × 0.2–0.5 cm, cylindrical, sometimes with basal mycelium and rarely subbulbous. Texture fibrous-cartilaginous, not fragile; surface longitudinally striated in the upper third, pruinose or fibrillose below, with more pronounced longitudinal striations in dry specimens. Internally yellowish, cerulescent, hollow; surface initially white to light brown, concolorous with the pileus, later yellowish brown and cerulescent. *Context* 0.2 cm thick, fleshy, creamy white (3A2; yellowish white), cerulescent. *Veil* absent. *Spore print* dark violet to blackish. *Basidiospores* (8.7–)11.5–16.1(–17.8) × (6.4–)7.8–11.7(–12.7) × (4.2–)5.6–9.8(–12.7) µm, Q= 1.33–1.87, Q_m= 1.59, lemon-shaped to

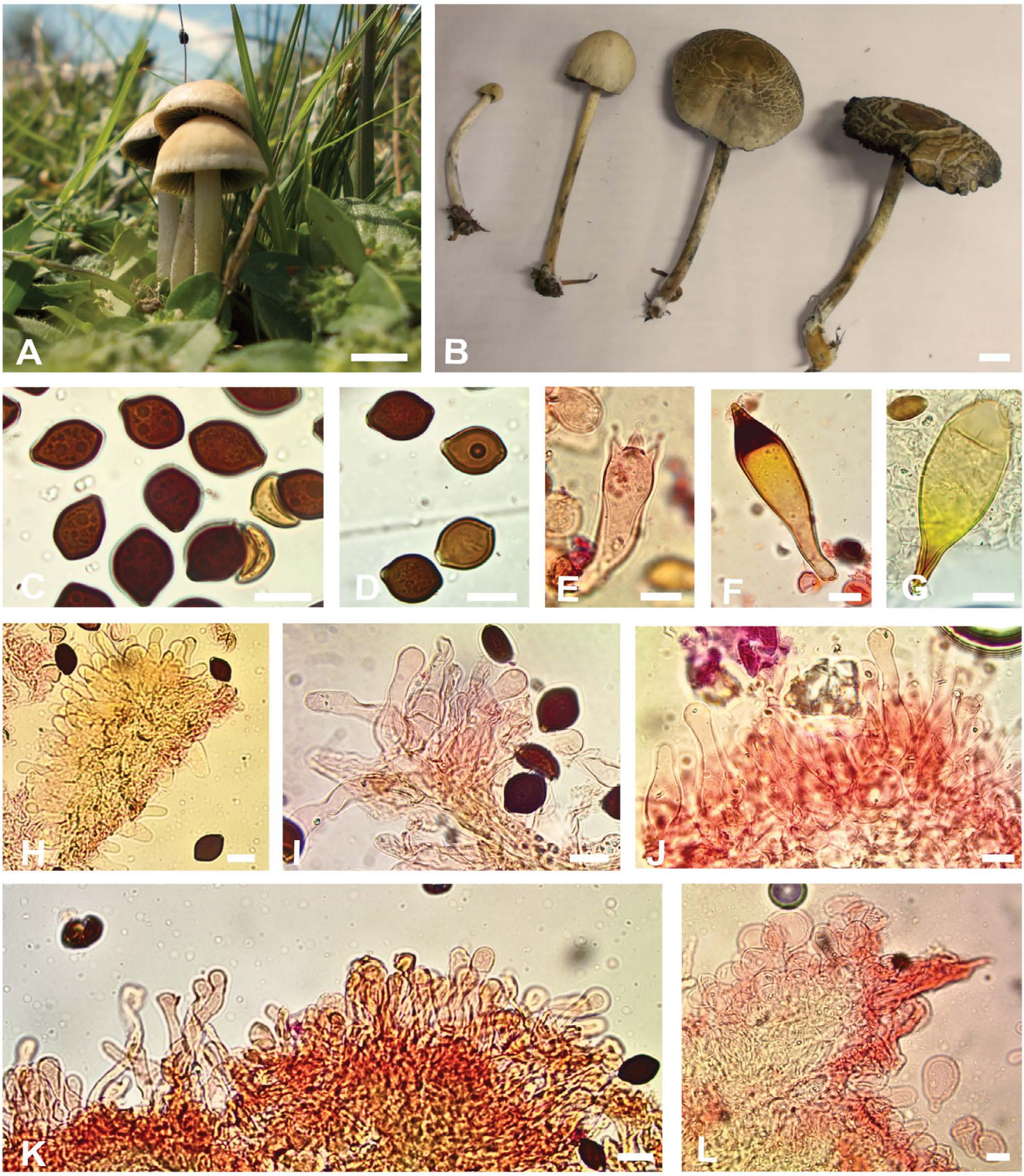

Fig. 5. *Panaeolus cyanescens*. Basidomata. **A.** MVHC 5765. **B.** MVHC 5818. Basidiospores. **C, D.** MVHC 5769. Basidia. **E.** MVHC 5828. Pleurocystidia. **F.** MVHC 5777. **G.** MVHC 5820. Cheilocystidia. **H, I.** MVHC 5841. **J.** MVHC 5824. Caulocystidia. **K.** MVHC 5838. Pileocystida. **L.** MVHC 5829. Scale bars: A, B = 1 cm, C–L = 10 µm.

hexagonal in frontal view and ellipsoidal in lateral view, light brown to commonly coffee-colored, smooth, with a wall thickness of 1.2–1.3 µm, and a conspicuous truncate germ pore up to 2.5 µm. *Basidia* 12.3–40.2 × 4.9–15.8 µm, cushion-shapped or clavate, tetrasporic. *Pleurocystidia* 45.3–83.5 × 12.8–22.5 µm, abundant, chrysocystidia, metuloid, and occasionally subfusoid, with thick walls or apical granulations. *Cheilocystidia* 12.7–56.7 × 3.4–21.8 µm, hyaline, thin-walled, polymorphic, appearing lageniform, cylindrical, or pyriform, with a subcapitate or slightly inflated apex. *Hymenophoral trama* composed of smooth hyphae, regularly arranged, up to 11 µm wide. *Pileipellis* formed by an epithelium of subglobose, hyaline, thin-walled cells, 17.2–42.5 × 13.6–31.8 µm. *Pileocystidia* hyaline, thin-walled, cylindrical, 22.8–96 × 6.4–36.2 µm. *Stipitipellis* a cutis composed of longitudinally arranged, yellowish-brown hyphae, up to 14 µm wide. *Caulocystidia* 18.7–50.5 × 3.6–17.3 µm, polymorphic, cylindrical, pedunculated spheroid, subclavate, or lageniform.

Specimens examined: **Uruguay**, Cerro Largo, Paso del Centurión, S32°8'28.9458", W53°43'51.276", 75 m.a.s.l., forest ecosystem, from cow dung, 1 Apr. 2021, *B. Corallo* (MVHC 5768 and MVHC 5769); Colonia, S33°58'23.4", W57°16'56.7", 20 m.a.s.l., open meadow with cattle, on horse dung, 8 Feb. 2022, *G. Morera et al.* (MVHC 5777); Maldonado, Sierra de las Ánimas, S34°36', W55°17', 209 m.a.s.l., on cow dung, 23 Mar. 2021, *G. Morera* & *S. Lupo* (MVHC 5765); 3 Mar. 2022, *G. Morera* & *S. Lupo* (MVHC 5816-18, MVHC 5820-5821, MVHC 5823-24, MVHC 5827-5832, MVHC 5834, MVHC 5837-44, MVHC 5846 and MVHC 5847); Maldonado, Sierra de las Ánimas, S34°42'12", W55°14'07, 75 m.a.s.l., on cow dung, 20 Mar. 2024, *S. Lupo* (MVHC 5879 and MVHC 5880).

Habit, habitat and distribution: Cosmopolitan distribution, in all continents except for Antarctica (Gerhardt 1996, Silva-Filho *et al*. 2019). This is the first record of this species for Uruguay. It was found in grasslands within fertilized fields, growing either around or directly on cow dung. It occurs solitarily or gregariously, forming groups of up to 13 specimens.

Notes: In the original description of *Agaricus cyanescens* (Berkeley & Broome 1871), the species was characterized by a dirty whitish to yellowish hemispherical cap, a stipe with a rooting base, and a pronounced cerulescent reaction occurring in various parts of the basidiome. For several decades, the species was segregated into the genus *Copelandia*, primarily due to its intense cerulescent staining and the presence of golden metuloid cystidia with acute apices (Young *et al.* 1989). However, recent molecular phylogenetic analyses have consistently recovered this taxon within *Panaeolus* (Hu *et al.* 2020, Asif *et al.* 2023, Voto & Angelini 2024, Consiglio & Marchetti 2025), thereby supporting its current generic placement. *Panaeolus cyanescens* exhibits a broad, cosmopolitan distribution, with confirmed occurrences across Europe, Africa, Oceania, Asia, and the Americas (Strauss *et al.* 2023). In South America, it has been recorded from Argentina (Batista *et al.* 2025) and Brazil (Singer 1986, Young 1989, Silva-Filho *et al.* 2018). The present study provides the first confirmed record of the species from Uruguay. Morphologically, the species is distinguished by a conical to campanulate pileus that may become broadly convex with age, typically pallid brown to yellowish white, sometimes with blue staining and deep erosions. Lamellae are dark gray to blackish and mottled. The stipe may display basal mycelium forming a pseudorhiza and consistently stains blue when bruised. Basidiospores are light brown to coffee-colored, lemon-shaped to hexagonal in frontal view, and ellipsoid in lateral view. Pleurocystidia are abundant and include both chrysocystidia and metuloid types. Macroscopic and microscopic features correspond closely with previous descriptions and illustrations (Saccardo 1887, Singer 1960, Guzmán & Petrarca 1972, Young 1989, Gerhardt 1996, Consiglio & Marchetti 2025). Nonetheless, certain differences have been noted: Singer (1960) observed slightly longer basidiospores and greater pileocystidial variation were described by Young (1989) documented metuloid caulocystidia; and basidomata in Consiglio & Marchetti (2025) were notably more pigmented. Basidiospore dimensions reported in the literature show some degree of variability: 13.0–15.0 × 10–12.0 µm (Bresadola 1912); 11.0–16 × 9.0–12.0 µm (Bresadola 1931); 11.0–13.0(–14.0) × 7.0–9.0 µm (Smith 1948); 13.0–14.0(–19.0) × 8.8–11.0 µm (Singer 1960); 12.0–14.0 × 8.5–11.0 µm (Oláh 1969); and 12.2–14.2 × 7.7–10.6 × 6.0–8.6 µm (Consiglio & Marchetti 2025). These differences may reflect phenotypic plasticity or underlying genetic variation within the species. Two species present in the Neotropics: *Panaeolus cambodginiensis* and *Pa. tropicalis*, can be distinguished by their smaller basidiospores, i.e.: 10–12.5 × 6.5–9 µm and 9–12 × 7–10 µm, respectively (Kaur *et al.* 2014, Batista *et al*. 2025). Additionally, *Pa. cyanescens* differs from *Pa. bisporus* in possessing four-spored basidia (Gerhardt 1996). With respect to psychoactive properties, *Pa. cyanescens* is unequivocally hallucinogenic and ranks among the species with some of the highest documented tryptamine concentrations, reaching up to 2.5 % of the dry fungal biomass (Guzmán 1959, Laussmann & Meier-Giebing 2010, Gotvaldová *et al*. 2022, Cohen *et al.* 2025).

Panaeolus foenisecii (Pers.) J. Schröt., *Botaniste* **17**(1–4): 187. 1926. Fig. 6A–G.

Description: *Pileus* 1–1.5 × 1.5–2.5 cm, conical to conical-campanulate; surface opaque, glabrous, smooth, occasionally with radial striations, dry to moist, not entirely hygrophanous. uniform coffee color (5D6; Light Brown) with a slightly darker center (5E6; Yellowish Brown), fading towards the margin. *Margin* straight to slightly incurved, entire, concolorous with the surface. *Lamellae* adnate, close, dark brown (5F8; Yellowish Brown), mottled. Edge entire, smooth, and light brown. *Stipe* 3–5.5 × 0.2 cm, central, cylindrical, with a smooth to pruinose surface, sometimes with longitudinal striations; fibrous and fragile in consistency, concolorous with the pileus surface, slightly lighter inside. *Context* up to 0.1 cm thick, fibrous, light brown (3A2; Yellowish White). *Veil* absent. *Spore print* dark brownish black. *Basidiospores* (12.2–)13–17.1(–19.5) × (6.4–)6.7–9.2(–9.3) × (5.7–)6.3–9.3(–9.4) µm, Q= 1.93–2.13, Q_m= 2, ellipsoid, flattened in lateral view, greenish-brown, walls up to 1.3 µm thick, with a rough ornamentation and a noticeable germ pore 1.5–2 µm. *Basidia* 21.3–29.9 × 10–11.6 µm, cushion-shaped, ventricose, hyaline, tetrasporic. *Pleurocystidia* absent. *Cheilocystidia* hyaline, subcylindrical to subventricose, 12.4–56.6 × 4.3–10.8 µm. *Hymenophoral trama* composed of smooth, hyaline, thin-walled hyphae, cylindrical, up to 5.5 µm diam. *Pileipellis* composed of a matrix of inflated, interwoven hyphae in brownish and greenish tones (21.1–39.6 × 17.6–21.4 µm). *Stipitipellis* composed of a cutis of parallel, yellowish-brown hyphae, up to 8 µm diam. *Caulocystidia* hyaline, variable in shape, lageniform ventricose with thick walls (21.4–37.9 × 5.9–13.5 µm), commonly cylindrical with an obtuse apex (25.1–41.2 × 2.3–9.6 µm), and rarely irregular, 21.8 × 10.1 µm.

Specimen examined: **Uruguay**, Lavalleja, surroundings of the "Salto del Penitente", S34°22'20", W55°03'10", 240 m.a.s.l., on horse dung, 23 May 2022, *G. Morera* & *S. Lupo* (MVHC 5862).

Habit, habitat and distribution: Cosmopolitan, commonly found in temperate grasslands across all continents except Asia and Antarctica (Gerhardt 1996). This is the first record

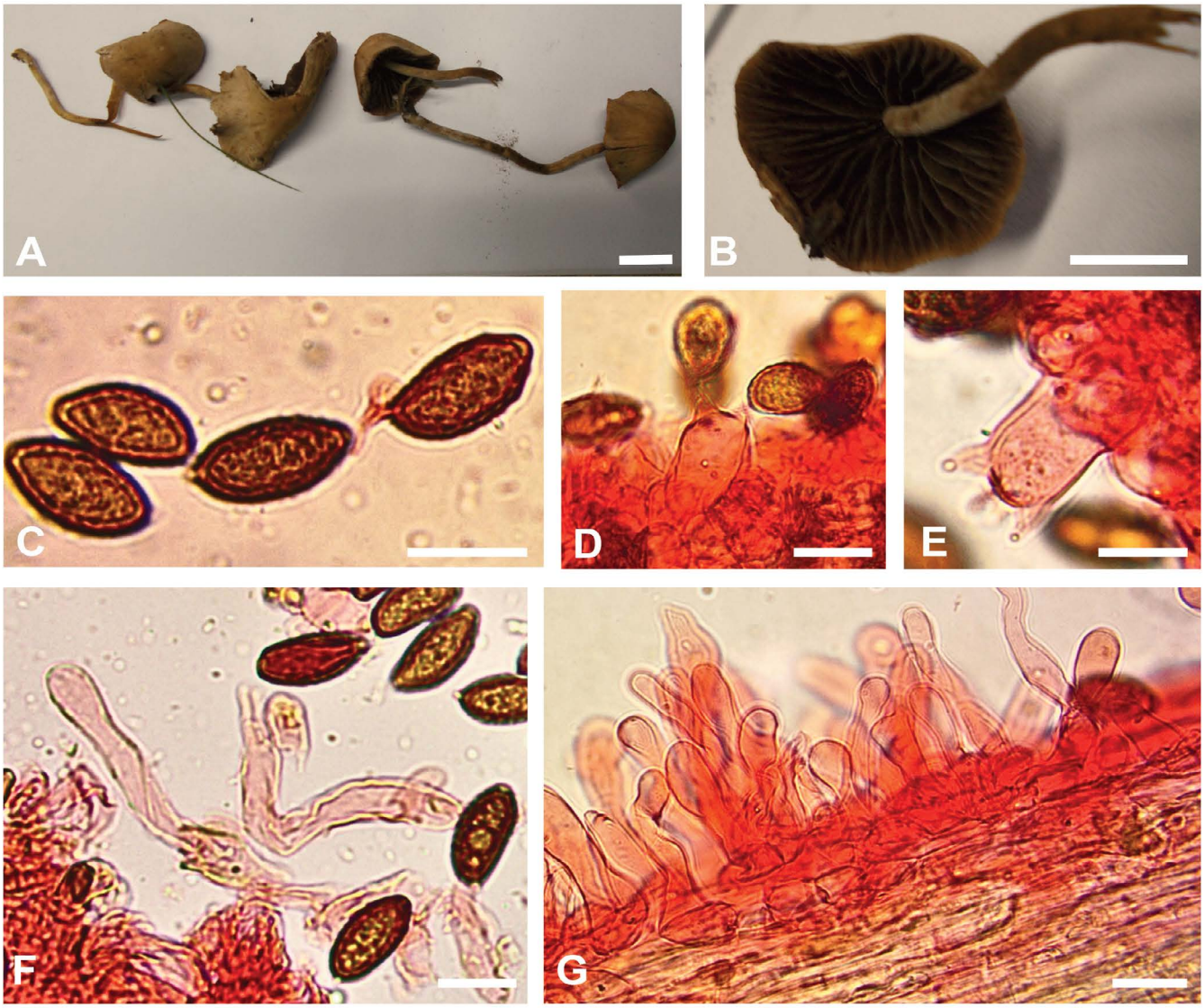

Fig. 6. *Panaeolus foenisecii* MVHC 5862. **A, B.** Basidomata. **C.** Basidiospores. **D, E.** Basidia. **F.** Cheilocystida. **G.** Caulocystidia. Scale bars: A, B = 1 cm, C–G = 10 µm.

for Uruguay of this species, found growing gregariously on horse dung, with groups of up to four specimens.

Notes: *Panaeolus foenisecii* was originally described from Germany under the name *Agaricus foenisecii* (Persoon 1801), and was historically classified in the genus *Panaeolina*, established by Maire (1933), due to its verrucose basidiospores (Singer 1986, Young 1989, Guzmán & Petrarca 1972). According to Gerhardt (1996), its distribution includes Europe, Africa, the Americas, and Australia, a pattern further corroborated by phylogenetic analysis of Consiglio & Marchetti (2025). The species typically grows on cow dung and fertilized soils, often found in parks, gardens, or grasslands (Persoon 1801, Consiglio & Marchetti 2025). It is morphologically distinguished by its conical to conical-campanulate pileus, brownish surface, brown spore print, and ornamented basidiospores that appear flattened on one side in lateral view (12.2–19.5 × 5.7–9.4 µm). The cystidia are hyaline and variable in shape, though consistently non-pigmented. The specimen MVHC 5862, collected in Uruguay on horse dung, was recovered in a distinct clade (BPP: 1, BS: 99) from those of the North Hemisphere analyzed by Consiglio & Marchetti (2025) (Fig. 1). Descriptions, figures and illustrations from European (Consiglio & Marchetti 2025; Young 1989), Mexican (Guzmán & Petrarca 1972), and Chinese specimens (He et al. 2026), including measurements of microscopic structures, broadly overlap with our observations. The Uruguayan specimen deviates from the traditional species description in having less polymorphic cheilocystidia (Consiglio & Marchetti 2025) and lacking the pleurocystidia reported by Guzmán and Petrarca (1972). *Panaeolus foenisecii,* like *Pa. olivaceous*, has verrucose basidiospores; however, the two species can be distinguished by their phylogenetic delimitation (Fig. 1), and by their distribution, which is more restricted in the case of *Pa. olivaceous* (Gerhardt 1996). A recently described species from China, *Pa. subfoenisecii*, appears to be closely related with *Pa. foenisecii*, however, this species is characterized by smooth and smaller basidiospores measuring 11.1–12.8 × 6.5–8.3 µm (He *et al*. 2026). Further collections are required to assess whether these differences lie within the intraspecific variation of the species or represent a distinct

taxon. Regarding its potential psychoactivity, *Pa. foenisecii* is considered a non-hallucinogenic species. Although latent psilocybin content has been reported (Ola'h 1969), this claim has been discussed, and many positive findings may have resulted from misidentifications or confusion with other species such as *Pa. subbalteatus* and/or *Pa. castaneifolius* (Stijve 1995). The studied specimen MVHC 5862 did not show significant contents of PSB or PS (Table 1), and based on a thorough review of the literature, *Pa. foenisecii* should be considered non-psychoactive (Allen 2010, Gotvaldová *et al*. 2022).

Panaeolus retirugis (Fr.) Gillet, *Hyménomycètes*: 621. 1878. Fig. 7A–L.

Description: *Pileus* 1.5–2 × 1.5 cm, conical-campanulate, umbonate; surface shiny or opaque, dry, not hygrophanous, glabrous, with radial or lacunar rugose ornamentation. Color light brown (5C7; Yellowish brown) fading to creamy whitish (4A3; Pale yellow) towards the margin. *Margin* incurved, serrated to eroded, appendiculate, concolorous with the surface. *Lamellae* adnexed, close, with blackish faces (4F5 to 4F3; Olive brown), waxy, and edges concolorous with the face or slightly whitish. *Stipe* 6–9 × 0.2–0.3 cm, central, cylindrical to subbulbous, with pruinose surface at the apex, then fibrillose. Texture fleshy to fibrous, whitish internally, and light brown externally, concolorous with the pileus, later dark with pinkish tones (8F8; Dark brown). *Context* 0.1 cm, fleshy, whitish. *Veil* absent. *Spore print* black. *Basidiospores* (10.2–)12.9–16.6(–17.1) × (7.5–)8.5–11.2(–12) × (4.4–)5.8–9.3(–10.1) µm, *Q* = 1.5–1.86, Q_m = 1.6, lemon-shaped to subhexagonal in frontal view, and ellipsoid in lateral view, with a slightly flattened side, light to dark brown, smooth, walls 0.8–1.2 µm thick and a prominent, truncate germ pore up to 2.5 µm diam. *Basidia* 15.4–41.5 × 6.1–14.6 µm, shortly clavate to clavate, to utriform with a central constriction, granulated, tetrasporic. *Pleurocystidia* not observed. *Cheilocystidia* 13.5–33.6 × 2.6–11.8 µm, cylindrical and tortuous to lageniform and ventricose, occasionally subcapitate at the apex, hyaline. *Hymenophoral trama* composed of smooth, inflated hyphae, up to 6 µm wide. *Pileipellis* composed of a palisade of pedunculated spheroid to ampulliform or isodiametric hyphae (hymenodermis), measuring 18.7–47.6 × 8–30.9 µm. *Pileocystidia* 30.4–66.8 × 10.7–47 µm, clavate or irregular, hyaline. *Pileus trama* consisting of interwoven, inflated hyphae up to 20 µm wide and filamentous hyphae up to 4 µm diam. *Stipitipellis* composed of a cutis of parallel, yellowish brown to greenish hyphae up to 5 µm wide. *Caulocystidia* 20.5–59.8 × 2.1–10.7 µm, hyaline, cylindrical, and very abundant.

Specimens examined: **Uruguay**, Lavalleja, surroundings of the "Salto del Penitente", S34°22'20", W55°03'10", 240 m.a.s.l., on horse dung, 23 May 2022, *G. Morera* & *S. Lupo* (MVHC 5857 and MVHC 5863); Colonia, S33°58'23.4", W57°16'56.7", 20 m.a.s.l., open meadow with cattle, on horse dung, 8 Feb. 2022, *G. Morera et al.* (MVHC 5776, MVHC 5782 and MVHC 5797).

Habit, habitat and distribution: Widely distributed in temperate regions of Europe and America (Guzmán & Petrarca 1972, Voto & Angelini 2024). This constitutes the first record for Uruguay. Found in fertilized meadow fields or on cow dung, occurring solitarily or in small groups of up to two specimens.

Notes: *Panaeolus retirugis* was originally described from Europe (Fries 1836-1838, Gillet 1878). It is currently understood to have a subcosmopolitan distribution across the Americas and Europe. The species has a complex taxonomic history, having been historically confused with *Pa. papilionaceus* and related species such as *Pa. sphinctrinus*, and *Pa. acuminatus* (Guzmán & Petrarca 1972, Voto & Angelini 2024). Recently, two paratypes specimens of *Pa. papilionaceus* var. *parvisporus* collected in the type locality in Germany, microscopically similar to *Pa. retirugis*, were included in the phylogenetic analyses conforming a clade -including specimens identified as *Pa. retirugis,* which was named *Pa. parvisporus* (Voto & Angelini 2024). Parallelly, it was shown that the holotype of *Pa. papilionaceus* var. *parvisporus*, grouped phylogenetically with *Pa. papilionaceus* sensu stricto while *Pa. retirugis* was recovered as an independent lineage (Consiglio & Marchetti 2025), in the same way that it is recovered in our analyses (Fig. 1, Clade D). Morphologically, *Pa. retirugis* is characterized by conical-campanulate, umbonate basidiomata with a light brown surface and distinct radial or lacunar rugose ornamentation. The pileus margin often bears remnants of the partial veil. Basidiospores measure on average 14.8 × 9.9 × 7.6 µm, are lemon-shaped to subhexagonal in frontal view, ellipsoid in lateral view, with slightly flattened walls. Cheilo- and caulocystidia present, the latter reaching up to 60 µm in length, and lacks pleurocystidia. This description agrees closely with those recently provided for the species (Voto & Angelini 2024, Consiglio & Marchetti 2025). *Panaeolus retirugis* differs from *Pa. pantropicalis* by the latter's deeper pileus fissures, smaller basidiospores (averaging up to 13 µm), and smaller cheilocystidia (up to 40 µm). *Panaeolus papilionaceus*, on the other hand, produces larger basidiospores [13.0–18.5(–19.0) × 8.5–13.0 × 7.0–10.0 µm] and belongs to a distinct clade (Fig. 1). *Panaeolus desertorum* develops secotioid basidiomata, while *Pa. punjabensis* differs by exhibiting bluing when handled, lacking an umbonate pileus and veil remnants, and producing fusiform basidiospores (Malysheva *et al*. 2019, Asif *et al.* 2023). According to our results, *Pa. retirugis* lacks PSB and PS (Table 1). It has been reported that *Pa. retirugis* may produce anesthetic effects on nervous tissue, suggesting the presence of other bioactive compounds (Guzmán & Petrarca 1972); however, these findings must be interpreted with caution due to the lack of molecular and detailed morphological data, and the historical confusion with closely related species, as discussed above.

Psilocybe cubensis (Earle) Singer, *Sydowia* **2**(1–6): 37. 1948. Fig. 8A–L.

Description: *Pileus* 50–120 × 10–25 mm, conical, conico-campanulate, or campanulate, becoming convex to plane at maturity, occasionally with an umbo or papilla; surface smooth, opaque to slightly shiny, glabrous, dry to subviscid, non-hygrophanous, yellowish brown (4A5, Light Yellow) fading towards the margin, becoming darker at maturity (6D7, Light Brown), occasionally with whitish scales when

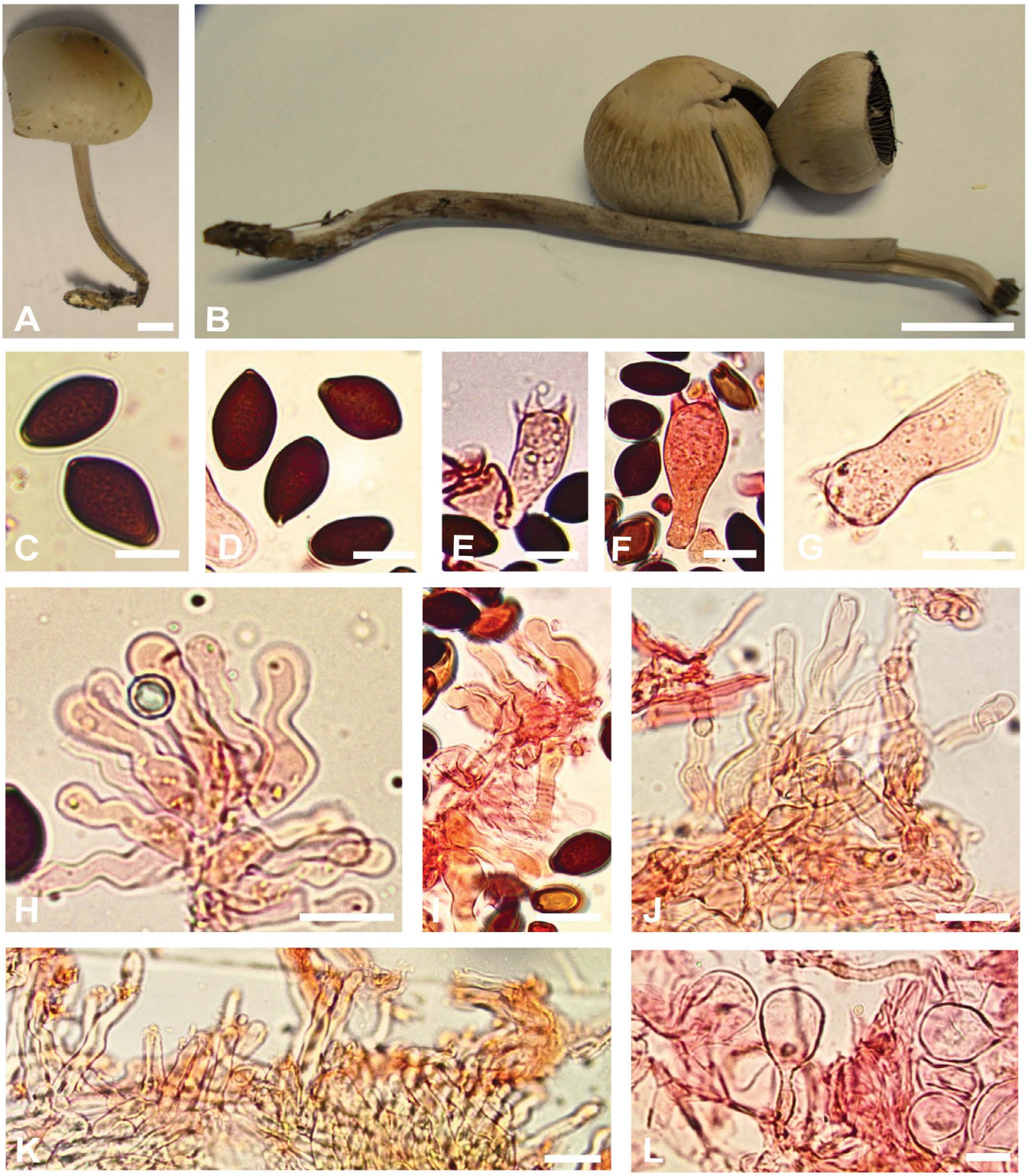

Fig. 7. *Panaeolus retirugis*. Basidomata. **A.** MVHC 5776. **B.** MVHC 5857. Basidiospores. **C.** MVHC 5776. **D.** MVHC 5797. Basidia. **E, F.** MVHC 5776. **G.** MVHC 5797. Cheilocystida. **H, I.** MVHC 5776. **J.** MVHC 5797. Caulocystidia **K.** MVHC 5776. Pileocystida. **L.** MVHC 5776. Scale bars: A, B = 1 cm, C–L = 10 µm.

Fig. 8. *Psilocybe cubensis*. Basidomata. **A, B.** MVHC 5853. Basidiospores. **C.** MVHC 5763. **D, E.** MVHC 5853. Basidia. **F.** MVHC 5762. **G.** MVHC 5851. Pleurocystidi. **H.** MVHC 5849. **I.** MVHC 5851. **J.** MVHC 5850. Cheilocystidia. **K.** MVHC 5762. **L.** MVHC 5850. Scale bars: A, B = 1 cm, C–L = 10 µm.

mature. *Margin* entire, concolorous with the surface or whitish. *Lamellae* light to dark brown (4A2, Yellowish White), turning dark purplish black at maturity (10F5, Purplish Brown), occasionally mottled; adnate to adnexed, close, with an entire whitish edge. *Stipe* 50–120 × 5–25 mm, cylindrical, thickened towards the base, with a bulbous base; white, shiny, turning bluish when bruised; longitudinally striate, fibrous. *Context* up to 20 mm thick, white, fleshy to corky, bluish upon bruising. *Veil* membranous, persistent to absent; may turn bluish but typically appears colored due to spore deposition once the pileus expands. *Spore print* dark purplish. *Basidiospores* (10–)10.4–14.5(–15.4) × (5.8–)6.3–9.2(–9.5) × (5.4–)5.6–8.9(–9.2) µm, *Q* = 1.57–1.77, Q_m = 1.67. Subhexagonal to hexagonal in frontal view, ellipsoid to oblong in lateral view, yellowish-brown, with thick walls up to 1.5 µm, and a conspicuous germ pore up to 2 µm wide. *Basidia* 12.7–37 × 4.8–12.7 µm, cylindrical to clavate, occasionally subutriform, sometimes with a median constriction, hyaline, occasionally granular, and tetrasterigmatic. *Pleurocystidia* 10.1–42.7 × 4.3–14.1 µm, clavate to fusiform, sometimes more ventricose, occasionally subglobose 7.7–22.5 × 5.7–14 µm, hyaline, with apical incrustation, thin-walled. *Cheilocystidia* 13.4–36 × 4.3–10.5 µm, lageniform with short to long necks, sometimes with a subcapitate apex, thin-walled, hyaline. *Hymenophoral trama* regular, composed of hyaline hyphae up to 7 µm wide. *Subhymenium* composed of inflated hyaline hyphae up to 9 µm wide. *Pileus trama* composed of filamentous hyphae up to 8 µm wide. *Pileipellis* an ixocutis of filamentous hyaline hyphae up to 7 µm wide. *Stipitipellis* composed of parallel hyaline hyphae up to 7.5 µm wide.

Specimens examined: **Uruguay**, Lavalleja, surroundings of the "Salto del Penitente", S34°22'20", W55°03'10", 240 m.a.s.l., on horse dung, 23 May 2022, *G. Morera* & *S. Lupo* (MVHC 5856); Rocha, Bosque de Ombúes, S34°22'8.4", W53°52'48.7", 10 m.a.s.l., 3 Apr. 2018, *G. Morera* & *S. Lupo* (MVHC 5763), 5 May 2022, *G. Morera* & *S. Lupo* (MVHC 5849-53); Montevideo, from anonymous users, Apr. 2021, (MVHC 5762 and MVHC 5764).

Habit, habitat and distribution: With a pantropical distribution (Guzmán 1983, Guzmán 1995), this species was previously recorded in Uruguay (Sequeira 2013). Characteristically, it grows on cow dung, occurring either solitarily or gregariously in groups of up to 4–5 specimens.

Notes: In 1906, Earle described the species *Stropharia cubensis*, which was later transferred to the genus *Psilocybe* by Singer (1948). This species has a broad distribution, typically growing on bovine and horse dung, or, more rarely, in rich pasture soils. *Psilocybe cubensis* is one of the most widely known and cultivated PSB-containing mushrooms worldwide, due to its psychoactive effects (Hawksworth & Wiltshire 2011, Gotvaldová *et al*. 2022). Uruguayan specimens exhibit robust basidiomata (up to 12 cm in pileus diam.), with a conical to plane pileus, occasionally presenting an umbo. The pileus surface is glabrous, yellowish brown, while the lamellae become dark purplish black at maturity. The stipe is white, sometimes slightly discolored, and bruises bluish when handled. Microscopically, the species is characterized by basidiospores measuring 10–15.4 × 5.8–9.5 × 5.4–9.2 µm, subhexagonal to hexagonal in frontal view, ellipsoid to oblong in lateral view, and yellowish-brown in color. Pleurocystidia are variable, while cheilocystidia are lageniform with short to long necks (with pileocystidia and caulocystidia absent). These features are consistent with previous descriptions by Singer & Smith (1958), Wright & Albertó (2002), Batista *et al.* (2025), and the phylogenetic placement established by Ramírez-Cruz *et al.* (2013). Singer & Smith (1958) and Batista *et al.* (2025) reported longer basidiospores, reaching up to 17 µm in length. Notably the sequence of the specimen Guzman 35102, corresponding to *Ps. subcubensis* in Ramírez-Cruz *et al.* (2013), clusters within our *Ps. cubensis* clade (BPP: 0.77, BS: 83; Fig. 2). Several studies have suggested that the only distinguishing feature between *Ps. cubensis* and *Ps. subcubensis* is the size of the basidiospores. However, in addition to phylogenetic evidence, we have observed a significant overlap in spore size of our specimens with the measurements documented for *Ps. subcubensis* by Guzmán (1995), Keller *et al*. (1999), and Guzmán *et al*. (2014), suggesting that *Ps. subcubensis* could be considered a synonym of *Ps. cubensis* in future taxonomic revisions. *Psilocybe natalensis* and *Ps. maluti* are phylogenetically related species, but the former differs by its smaller spore size (8.8–10.1 × 5.5–6.0 µm), as documented by Windsor *et al.* (2025), while the latter exhibits a secotioid habit (Van Der Merwe *et al.* 2024). Additionally, *Psilocybe chuxiongensis* is extremely similar in macromorphology to *Ps. cubensis* but differs by lacking an annulus and being reported exclusively from China (Ma *et al.* 2014). The samples analyzed in Uruguay showed a wide range of variation in tryptamine content, reaching a maximum of 0.91% (PSB + PS) of dry weight in MVHC 5849 (Table 1).

Psilocybe stuntzii Guzmán & J. Ott, *Mycologia* **68**(6): 1261. 1977. [1976]. Fig. 9A–J.

Description: *Pileus* 10–25 × 3–15 mm, conical, almost hemispherical to plano-convex, with a well-defined umbo, papilla-like; surface smooth, shiny, translucent-striate, glabrous, nearly viscid when moist, hygrophanous, yellowish brown (5D6; Light Brown) to dark or olive-brown (4F8; Olive Brown), homogeneous or with a darker center and lighter sectors. *Margin* entire to eroded, striate, concolorous with the surface, olive-brown, hygrophanous, cerulescent. *Lamellae* non-homogeneous brown (6D6; Dark Brown) with violet mottling, adnexed, close, edge irregular and concolorous with the face. *Stipe* 10–50 × 1–4 mm, cylindrical, straight to sinuous, tapering towards the base, hollow, yellowish-brown to dark brown (5E6; Yellowish Brown); semi-translucent when moist, base concrescent, with fibrillose surface and longitudinal striations, fibrous, bearing cerulescent mycelial projections. *Veil* membranous, persistent, cerulescent. *Context* 1–2 mm, gummy, whitish to brownish, concolorous with the stipe, cerulescent. *Spore print* dark violet. *Basidiospores* (7.9–)9–12.3(–13.4) × (4.1–)5.2–7.6(–8.3) × (4.4–)5–7.4(–7.8) µm, *Q*= 1.52–1.85, Q_m= 1.69, ellipsoid, subangular to subrhomboid in frontal view, ellipsoid to oblong in lateral view, yellowish-brown, with thick walls up to 1.2 µm and a conspicuous germ pore up to 1.7 µm. *Basidia* 9.4–32.1 × 4.5–11.8 µm, cylindrical to clavate, sometimes with a median constriction, hyaline,

Fig. 9. *Psilocybe stuntzii.* Basidomata. **A.** MVHC 5854. **B.** MVHC 5855. Basidiospores. **C, D.** MVHC 5854. Basidia. **E.** MVHC 5858. Cheilocystida. **F**. MVHC 5858. **G.** MVHC 5874. **H.** MVHC 5858. Caulocystidia. **I, J.** MVHC 5870. Scale bars: A, B = 1 cm, C-J = 10 µm.

occasionally granular, bi- to tetrasporic. *Pleurocystidia* absent. *Cheilocystidia* 12.3–33.8 × 2.9–10.2 µm, lageniform with a long neck, occasionally with a short neck, sometimes cylindrical or ventricose; apex with refractive content, occasionally bifurcated; hyaline. *Hymenophoral trama* regular, composed of hyaline hyphae up to 7 µm wide. *Subhymenium* with inflated hyaline hyphae up to 9 µm wide. *Pileal trama* composed of filamentous hyphae up to 5 µm wide. *Pileipellis* of hyaline hyphae up to 7 µm diam. *Stipitipellis* formed by parallel hyphae with incrustations, up to 5 µm wide. *Caulocystidia* 10.5–33.9 × 3.5–13.2 µm, lageniform with a long neck, sometimes bifurcated, hyaline. Clamp connections present.

Specimens examined: **Uruguay**, Lavalleja, surroundings of the "Salto del Penitente", S34°22'20", W55°03'10", 240 m.a.s.l., 23 May 2022, growing in manured soil, in fields with cattle, *G. Morera* & *S. Lupo* (MVHC 5854-55, MVHC 5858-61, MVHC 5864-66, MVHC 5869-5878).

Habit, habitat and distribution: *Psilocybe stuntzii* was previously only recorded from North America (Guzmán & Ott 1976) and is now reported for Uruguay, suggesting it may be an amphitropical species. It is associated with horse and cow dung and is often found growing in groups directly from the soil, with as many as eight specimens observed together.

Notes: *Psilocybe stuntzii* was described from Washington State (USA) as a common graminicolous species in the region, used recreationally due to its psychoactive properties (Guzmán & Ott 1976). It is characterized by a papillate, lustrous pileus that may exhibit light ochraceous tones, violaceous lamellae, and a bluish annulus. Microscopically, it has basidiospores measuring 8.2–12.6 × 6–7.7 × 5.5–6.6 µm, lentiform in frontal view and ellipsoid in side view, no pleurocystidia, and long-necked cheilocystidia up to 27.5 µm long. These characters match closely with those observed in Uruguayan specimens; however, another blue-ringed species with highly overlapping micromorphological features, *Ps. caeruleoannulata* (≡ *Ps. uruguayensis*), has previously been recorded from Uruguay and southern Brazil (Guzmán 1978, Silva 2013). It is possible that specimens described as *Ps. caeruleoannulata* from Uruguay actually belong to *Ps. stuntzii*; nevertheless, this hypothesis requires confirmation through including sequences of the holotype kept at BAFC herbarium in phylogenetic analyses, unfortunately we were unable to access the type materials. *Psilocybe semilanceata* is a related species, but differs in lacking a distinct bluish annulus and in having a wavy stipe (Cacialli *et al.* 1996). Regarding the alkaloid content, *Ps. stuntzii* has been reported as hallucinogenic, with psilocybin and psilocin concentrations below 1 % (Guzmán & Ott 1976, Windsor *et al*. 2025), and even lower levels have been recorded in specimens from Brazil and Uruguay (Stijve & Demeijer 1993, this work).

DISCUSSION

Recent advances in molecular studies of species diversity within the genera *Panaeolus* and *Psilocybe* have improved our understanding of their evolutionary relationships and have contributed to refining species circumscription and resolving species complexes (Ramírez-Cruz *et al.* 2013, Voto & Angelini 2024, Consiglio & Marchetti 2025, He *et al*. 2026). In this study, we sequenced and analyzed 57 *Panaeolus* and 16 *Psilocybe* Uruguayan specimens, placing them within phylogenies comprising 285 and 228 terminals, respectively, in order to determine their phylogenetic placement and relationships with previously documented taxa. To construct these phylogenies, the most widely represented loci were used for each genus: ITS and LSU for *Panaeolus*, and ITS, LSU, *rpb1*, and *tef1* for *Psilocybe*.

In *Panaeolus*, a total of 29 clades were recovered (Fig. 1), representing distinct lineages. Of these, 20 correspond to previously described species included in earlier phylogenies (Voto & Angelini 2024, Consiglio & Marchetti 2025), one represents a new species (described here), and eight clades correspond to species that have not yet been identified. Five of these clades, representing undescribed species, occupy basal positions in the phylogeny. Although several terminal clades were recovered in a pattern comparable to earlier studies, the overall topology is not fully congruent and remains difficult to compare with the most recent large-scale phylogenetic treatments (Voto & Angelini 2024, Consiglio & Marchetti 2025). Also, the subgenera proposed by He *et al.* (2026) are likewise not recovered, with the exception of subgenus *Panaeolus*, corresponding to our clade D (Fig. 1). These differences may be attributable, at least in part, to the broader taxon sampling incorporated in the present analyses, which nearly doubles the number of terminal taxa included in previous studies.

In the case of *Psilocybe*, the topology recovered terminal clades previously shown in multigen phylogenetic analyses (Ramirez-Cruz *et al.* 2013, Canan *et al.* 2024, Ostuni *et al.* 2024). In the phylogenetic tree of Fig. 2, we show four clades (A–D), within clade A, the three groups 'mexicanae', 'cordiosporae', and 'zapotecorum', each of which includes several representatives of *Psilocybe* sections sensu Guzmán (1983, 1995), represent more comprehensively sampled versions of what has been shown in previous works (Ramírez-Cruz *et al.* 2013). Within clade B two strongly supported groups can be recognized here named as 'semilanceatae' and 'atrobrunneae' according to *Psilocybe* sections of Guzmán (1983, 1995) and Singer (1986) respectively. Clade C includes two groups, here named as 'cyanescens' and 'serbica', corresponding with *Psilocybe* stirps sensu Singer (1986) and Noordeloos (2011) respectively. Finally, within clade D, two other strongly supported groups are recognized, one is congruent with previous works, *i.e.* 'cubensae' (Ramirez-Cruz *et al.* 2013) and the other, also recovered previously (Canan *et al.* 2024, Ostuni *et al.* 2024) is here named as 'subaeruginascens' (due *Ps. subaeruginascens* was the first described species in the group).

Combined morphological and phylogenetic analyses of Uruguayan specimens allowed the identification and description of five *Panaeolus* species, of which only *Pa. antillarum* had been previously recorded for Uruguay (Gerhardt 1996, Sequeira 2017). In turn, *Pa. retirugis* was likely previously misidentified as *Pa. papilionaceus* and *Pa. acuminatus* (Herter 1907, Felippone 1928, Rosa-Mato 1939), likely due to its affinities with this species. The remaining taxa — *Pa. cyanescens*, *Pa. charrua sp. nov*. and *Panaeolus foenisecii* — represent new records for the country, and

one also represents a new species to science. For *Psilocybe*, two species were found and described: *Psilocybe cubensis*, which had been previously recorded for Uruguay (Sequeira 2013), and *Ps. stuntzii*, which represents a novel record for the country. This taxon may previously have been confused with *Psilocybe caeruleoannulata* Singer ex Guzmán and/or *Ps. uruguayensis* Singer ex Guzmán (Guzmán 1978).

The contents of PS and PSB exhibited wide variation among species and samples, which may be attributed to differences in sample origin and to the intrinsic instability of tryptamines. PSB can be hydrolyzed to PS under acidic or humid conditions via endogenous phosphatases present in fungal tissues (Gartz 1994). In addition, it has been demonstrated that ground mushrooms stored under different conditions show significant loss of tryptamine content after one year, with storage in darkness at 20 °C being comparatively the most stable condition (Gotvaldová *et al*. 2021). The time elapsed between mushroom collection and chemical analysis is another factor likely contributing to PSB/PS variability (Bradshaw *et al*. 2022, Miller *et al*. 2024). For example, *Ps. stuntzii* showed only low levels of PS (up to 0.021 %), which are markedly lower than those reported in other studies (Windsor *et al.* 2025). However, these samples were analyzed after more than one year of storage, which likely contributed to reduced tryptamine contents. In *Ps. cubensis*, pooled specimens MVHC 5762, MVHC 5849 sample 2, and MVHC 5851 contained no detectable PSB and had been stored for over one year. In contrast, MVHC 5849 samples 1 and 3 and MVHC 5850, all stored for less than one year, contained PSB levels ranging from 0.41 to 0.71 %. An exception was MVHC 5853, which, despite being analyzed within one year, showed comparatively low contents of both PSB and PS. For *Pa. cyanescens*, all samples were analyzed within the collection year, with the exception of MVHC 5827, which exhibited the lowest tryptamine levels and was quantified two years after collection. In the remaining specimens, PSB content ranged from 0 to 0.28 %, while PS varied from 0.06 to 0.42 %. PSB and PS contents in *Psilocybe cubensis* are consistent with previously documented ranges, whereas *Pa. cyanescens* showed lower concentrations than those reported in previous studies (Gotvaldová *et al.* 2022).

No alkaloids were detected (<LOD) in *Pa. foenisecii*, *Pa. antillarum*, and *Pa. retirugis*, consistent with previous reports describing these taxa as non-psychoactive (Guzmán & Petrarca 1972, Allen 2010). In *Pa. charrua*, no PSB or PS was detected, however, given the lack of previous records, the time elapsed between collection and measurement, and the presence of closely related psychoactive species, we cannot exclude the possibility that this species may produce significant alkaloid contents under different conditions.

Regarding PSB and PS occurrence, these alkaloids were detected in 7 of the 29 phylogenetic species of *Panaeolus* recognized in Figure 1. In contrast, within *Psilocybe*, among the 42 recovered phylogenetic species (Fig. 2), only one (*Ps. atrobrunnea*) has been confirmed to lack PSB/PS production. It has been suggested that PSB/PS occurrence in *Panaeolus* is sporadic across the phylogeny, potentially resulting from an ancestral acquisition followed by multiple losses, or alternatively from independent acquisition events (Hu *et al*. 2020, Meyer & Slot 2023). However, as shown in Fig. 1, there is a notable clustering of producer species within Clade A. In contrast, the widespread distribution of PSB/PS production in *Psilocybe* supports the hypothesis of a single ancestral acquisition (Meyer & Slot 2023).

CONCLUSIONS

In the present study, we applied an integrative approach combining phylogenetic, morphological, and chemical analyses to investigate Uruguayan specimens of *Panaeolus* and *Psilocybe*. Seven species were documented. Within *Panaeolus*, five species were recognized, including *Pa.* antillarum, the only taxon previously recorded in Uruguay; three new country records (*Pa. cyanescens*, *Pa. foenisecii*, and *Pa. retirugis*); and one species new to science (*Pa. charrua*). Two *Psilocybe* species were identified: *Psilocybe cubensis*, previously reported from Uruguay, and *Ps. stuntzii*, representing a new national record and an extension of its known distribution. The discovery of several previously unrecorded taxa highlights the still underexplored fungal diversity of Uruguay and underscores the need for continued systematic studies. Among the studied taxa, only *Pa. cyanescens* and the two *Psilocybe* species tested positive for psychoactive alkaloids (PSB/PS). In the context of emerging regulations concerning fungi and their derivatives, these results provide an evidence-based framework for prioritizing species with confirmed alkaloid production in future scientific and regulatory efforts.

ACKNOWLEDGMENTS

The authors acknowledge the support of Agencia Nacional de Investigación e Innovación (POS_NAC_2022_1_174048), Comisión Académica de Posgrado (CAP), CSIC - Universidad de la República (Proyecto CSIC Grupos I+D, 1063), and PEDECIBA (Universidad de la República), as well as the Interdisciplinary Group on Psychedelic Studies Arché (arche.ei.udelar.edu.uy), for providing scholarships, funding, and an academic environment that enabled the development of this work. We also thank Michelle Geraldine Campi for kindly sharing occurrence records from Paraguay. We thank the anonymous reviewers and the editor for their valuable corrections and suggestions.

Conflict of interest The authors declare no conflicts of interest.

REFERENCES

Allen JW (2010). A Chemical Referral and Reference Guide to the Known Species of Psilocin and/or Psilocybin-containing Mushrooms and their Published Analysis and Bluing Reactions: An Updated and Revised List. https://www.researchgate.net/profile/John-Allen-45/publication/215476195

Allen JW, Sihanonth P, Gartz J, et al. (2024). An ethnopharmacological and ethnomycological update on the occurrence, use, cultivation of known species, chemical analysis, and SEM photography of neurotropic fungi from Thailand, Cambodia and other regions of South, Southeast Asia, Malaysia, Indonesia, and Bali. Ethnomycological Journals: Sacred Mushroom Studies 9: 1–201.

Angelini C, Voto P (2023). First record of Panaeolus sylvaticus in the Dominican Republic and notes on Panaeolus and Panaeolopsis. Mycological Observations 6: 22-29.

Asif M, Firdous Q, Izhar A, et al. (2023). Molecular and morphological studies reveal a new species of Panaeolus (Agaricales, Basidiomycota) from Punjab, Pakistan. European journal of taxonomy 888: 77–96. https://doi.org/10.5852/ejt.2023.888.2215

Batista AJ, Almirón HA, Forlin G, et al. (2025). Psilocybe cubensis y Panaeolus cyanescens (Basidiomycota, Agaricales), dos especies de hongos alucinógenos en el NE de Argentina. Boletín de la Sociedad Argentina de Botánica 60(1): 1–1. https://doi.org/10.31055/1851.2372.v60.n1.46185

Berkeley MJ, Broome CE. (1871). The Fungi of Ceylon. Journal of the Linnean Society of London, Botany, 11(56): 494–567. https://doi.org/10.1111/j.1095-8339.1871.tb00163.x

Borovička J, Rockefeller A, Werner PG (2012). Psilocybe allenii–a new bluing species from the Pacific Coast, USA. Czech Mycology 64(2): 181–195.

Borovička J, Oborník M, Stříbrný J (2015). Phylogenetic and chemical studies in the potential psychotropic species complex of Psilocybe atrobrunnea with taxonomic and nomenclatural notes. Persoonia-Molecular Phylogeny and Evolution of Fungi 34(1): 1–9. https://doi.org/10.3767/003158515X685283

Bradshaw AJ, Backman TA, Ramírez-Cruz V, et al. (2022). DNA authentication and chemical analysis of Psilocybe mushrooms reveal widespread misdeterminations in fungaria and inconsistencies in metabolites. Applied and Environmental Microbiology 88(24): e01498-22. https://doi.org/10.1128/aem.01498-22

Bradshaw AJ, Sharp C, Van Der Merwe B, et al. (2026). Discovery of the closest free-living relative of the domesticated 'magic mushroom' Psilocybe cubensis in Africa. Proceedings of the Royal Society B: Biological Sciences 293(2066): 20252270. https://doi.org/10.1098/rspb.2025.2270 .

Bresadola J (1912). Basidiomycetes philippinenses. Hedwigia 53: 46–80.

Bresadola J (1931). Iconographia mycologica. Società Botanica Italiana 18: 890–897.

Cacialli G, Caroti V, Doveri F (1996). Contributo allo studio dei funghi fimicoli-XI. Agaricales: Psilocybe semilanceata (Fries: Fries) Kummer e Pholiotina coprophila (Kühner) Singer. Funghi e Ambiente 72: 5–16.

Canan K, Ostuni S, Rockefeller A, et al. (2024). Psilocybe caeruleorhiza: a new, cold weather fruiting species of psilocybin containing mushroom from the Midwest in section Aztecorum. Journal of the American Amateur Mycologists: 1–16.

Carhart-Harris R, Giribaldi B, Watts R, et al. (2021). Trial of psilocybin versus escitalopram for depression. New England Journal of Medicine 384(15): 1402–1411. https://doi.org/10.1056/NEJMoa2032994

Cohen J, Sulimani L, Procaccia S, et al. (2025). Comprehensive analysis of 42 psilocybin-producing fungal strains reveals metabolite diversity and species-specific clusters. Scientific Reports 15(1): 13822.

Consiglio G, Marchetti M (2025). Contributo alla conoscenza del Genere Panaeolus sensu lato. Rivista di Micologia 66(3): 209–286.

Contu M. (1998). Un nouveau Gastéromycète de Sardaigne. Bulletin trimestriel de la Société Mycologique de France 114(1): 11–15.

De D, Perry BA (2017). Panaeolus antillarum (Basidiomycota, Psathyrellaceae) from wild elephant dung in Thailand. Current Research in Environmental & Applied Mycology. Journal of Fungal Biology 7(4): 275–281.

Dennis RWG (1961). Fungi venezuelani: IV. Agaricales. Kew Bulletin 15(1): 67–156.

Dix NJ, Webster J (1995). Coprophilous fungi. In: Fungal ecology (Dordrecht: Springer), Netherlands: 203–224.

Dörner S, Rogge K, Fricke J, et al. (2022). Genetic survey of Psilocybe natural products. ChemBioChem 23(14): e202200249. https://doi.org/10.1002/cbic.202200249

Doyle JJ, Doyle JL (1987). A rapid DNA isolation procedure for small quantities of fresh leaf tissue. Phytochemical Bulletin 19: 11–15.

Earle FS (1906). Algunos hongos cubanos. Informes Anuales de la Estación Central Agronómica de Cuba 1: 225–242.

Felippone F (1928). Contribution à la flore mycologique de l'Uruguay. Annales de Cryptogamie Exotique 1 (4): 338-348.

Fries EM (1821). Systema Mycologicum. Ex Officina Berlingiana, Lund, Sweden.

Fries EM (1828). Elenchus fungorum: sistens commentarium in Systema mycologicum (Vol. 1). Sumptibus E. Mauritii, Sweden.

Fries EM (1836–1838). Epicrisis Systematis Mycologici: seu synopsis hymenomycetum (Vol. 1). Sumptibus auctoris, Sweden.

Fries EM (1849). Summa vegetabilium Scandinaviae: seu enumeratio systematica et critica plantarum quum Cotyledonearum, tum Nemearum inter Mare Occidentale et Album, inter Eidoram et Nordkap, hactenus lectarum, indicata simul distributione geographica; accedunt expositio systematis plantarum morphologici, et mantissa synoptica. Sectio 2. Bonnier, Stockholm.

Garnica S, Weiss M, Walther G, et al. (2007). Reconstructing the evolution of agarics from nuclear gene sequences and basidiospore ultrastructure. Mycological Research 111(9): 1019–1029. https://doi.org/10.1016/j.mycres.2007.03.019

Gartz J (1994). Extraction and analysis of indole derivatives from fungal biomass. Journal of Basic Microbiology 34(1): 17–22. https://doi.org/10.1002/jobm.3620340104

Gerhardt E (1996). Taxonomische Revision der Gattungen Panaeolus and-Panaeolina (Fungi, Agaricales, Coprinaceae). Bibliotheca Botanica 147: 1–149.

Gillet CC (1878). Les champignons (fungi, hyménomycètes) qui croissent en France: description et iconographie, propriétés utiles ou vénéneuses. Lib. JB Baillière et Fils, France.

Gotvaldová K, Hájková K, Borovička J, et al. (2021). Stability of psilocybin and its four analogs in the biomass of the psychotropic mushroom Psilocybe cubensis. Drug testing and analysis 13(2): 439–446. https://doi.org/10.1002/dta.2950

Gotvaldová K, Borovička J, Hájková K, et al. (2022). Extensive collection of psychotropic mushrooms with determination of their tryptamine alkaloids. International Journal of Molecular Sciences 23(22): 14068. https://doi.org/10.3390/ijms232214068

Guzmán G (1959). Sinopsis de los conocimientos sobre los hongos alucinógenos mexicanos. Botanical Sciences 24: 14–34. https://doi.org/10.17129/botsci.1058

Guzmán G (1978). The species of Psilocybe known from Central and South America. Mycotaxon 7(2): 225–255.

Guzmán G (1983). The genus Psilocybe. A systematic revision of the known species including the history, distribution and chemistry of the hallucinogenic species. Beihefte zur Nova Hedwigia 74: 1–439.

Guzmán G (1995). Supplement to the monograph of the genus Psilocybe. Taxonomic monographs of Agaricales. Bibliotheca Mycologica 159: 91–141.

Guzmán G (2005). Species diversity in the genus Psilocybe (Basidiomycotina, Agaricales, Strophariaceae) of world mycobiota, with special attention to hallucinogenic properties. International Journal of Medicinal Mushrooms 7: 305.

Guzmán G, Ott J (1976). Description and chemical analysis of a new species of hallucinogenic Psilocybe from the Pacific Northwest. Mycologia 68(6): 1261–1267. https://doi.org/10.1080/00275514.1976.12020019

Guzmán G, Petrarca AP (1972). Las especies conocidas del género Panaeolus en México. Scientia Fungorum 6: 17–53. https://doi.org/10.33885/sf.1972.2.408

Guzmán G, Allen JW, Gartz J (1998). A worldwide geographical distribution of the neurotropic fungi, an analysis and discussion. Annali del Museo Civico di Rovereto 14: 189–280.

Guzmán G, Ramirez Guillen F, Hyde KD, et al. (2012). Psilocybe ss in Thailand: four new species and a review of previously recorded species. Mycotaxon 119(1): 65–81.

Guzmán G, Nixon SC, Ramírez-Guillén F, et al. (2014). Psilocybe s. str. (Agaricales, Strophariaceae) in Africa with description of a new species from the Congo. Mycotaxon 127: 237–249.

Haikazian S, Chen-Li DCJ, Johnson DE, et al. (2023). Psilocybin-assisted therapy for depression: A systematic review and meta-analysis. Psychiatry Research 329: 115531. https://doi.org/10.1016/j.psychres.2023.115531

Halberstadt AL, Geyer MA (2011). Multiple receptors contribute to the behavioral effects of indoleamine hallucinogens. Neuropharmacology 61(3): 364–381. https://doi.org/10.1016/j.neuropharm.2011.01.017

Hall TA (1999). BioEdit: a user-friendly biological sequence alignment editor and analysis program for Windows 95/98/NT. Nucleic acids symposium series 41(41): 95-98.

Hawksworth DL, Wiltshire PE (2011). Forensic mycology: the use of fungi in criminal investigations. Forensic Science International 206(1–3): 1–11. https://doi.org/10.1016/j.forsciint.2010.06.012

He MQ, Yang WQ, Phurbu D, et al. (2026). Systematic study of Panaeolus (Agaricales, Galeropsidaceae) sensu lato and psilocybin-producing traits of species from China. IMA Fungus 17: e167329. 10.3897/imafungus.17.167329

Herter W (1907). Hongos coleccionados en la República Oriental del Uruguay. Anales del Museo Nacional de Montevideo 2(1): 1–40.

Hesler LR (2013). Panaeolus Notebook 1. L.R. Hesler's Mushroom Notebooks. https://trace.tennessee.edu/utk_hesler/162

Høiland K (1978). The genus Psilocybe in Norway. Norwegian Journal of Botany 25: 111–122.

Højlund M, Kafali HY, Kırmızı B, et al. (2025). Efficacy, all-cause discontinuation, and safety of serotonergic psychedelics and MDMA to treat mental disorders: A living systematic review with meta-analysis. European Neuropsychopharmacology 101: 41–55. https://doi.org/10.1016/j.euroneuro.2025.09.011

Hoang DT, Chernomor O, Von Haeseler, et al. (2018). UFBoot2: improving the ultrafast bootstrap approximation. Molecular biology and evolution 35(2): 518-522.

Hu Y, Mortimer PE, Karunarathna SC, et al. (2020). A new species of Panaeolus (Agaricales, Basidiomycota) from Yunnan, Southwest China. Phytotaxa: 434(1): 22–34. https://doi.org/10.11646/phytotaxa.434.1.3

Hyde D (2014). Psilocybe chuxiongensis, a new bluing species from subtropical China. Phytotaxa 156(4): 211–220. https://doi.org/10.11646/phytotaxa.156.4.3

Hyde KD, Udayanga D, Manamgoda DS, et al. (2013). Incorporating molecular data in fungal systematics: a guide for aspiring researchers. arXiv: 1302.3244. https://doi.org/10.48550/arXiv.1302.3244

Kalyaanamoorthy S, Minh BQ, Wong TK, et al. (2017). ModelFinder: fast model selection for accurate phylogenetic estimates. Nature Methods 14(6): 587–589.

Katoh K, Rozewicki J, Yamada KD (2019). MAFFT online service: multiple sequence alignment, interactive sequence choice and visualization. Briefings in Bioinformatics 20(4): 1160–1166. https://doi.org/10.1093/bib/bbx108

Kaur A, Atri NS, Kaur M (2014). Two new species of Panaeolus (Psathyrellaceae, Agaricales) from coprophilous habitats of Punjab, India. Journal on New Biological Reports 3(2): 125–132.

Keller T, Schneider A, Regenscheit P, et al. (1999). Analysis of psilocybin and psilocin in Psilocybe subcubensis Guzman by ion mobility spectrometry and gas chromatography–mass spectrometry. Forensic Science International 99(2): 93–105. https://doi.org/10.1016/S0379-0738(98)00168-6

Kornerup A, Wanscher JH (1978). Methuen handbook of color (Third Edition. Eyre Methuen), London.

Kummer P (1871). Der Führer in die Pilzkunde: Anleitung zum methodischen, leichten und sichern Bestimmen der in Deutschland vorkommenden Pilze, mit Ausnahme der Schimmel- und allzu winzigen Schleim- und Kern-Pilzchen (Vol. 1. Buchhandlung), Zerbst: E. Luppe'sche.

Laussmann T, Meier-Giebing S (2010). Forensic analysis of hallucinogenic mushrooms and khat (Catha edulis Forsk) using cation-exchange liquid chromatography. Forensic Science International 195(1–3): 160–164. https://doi.org/10.1016/j.forsciint.2009.12.013

Lenz C, Wick J, Braga D, et al. (2020). Injury-triggered blueing reactions of Psilocybe "magic" mushrooms. Angewandte Chemie 132(4): 1466–1470. https://doi.org/10.1002/ange.201910175

Li H, Zhang H, Zhang Y, et al. (2020). Mushroom poisoning outbreaks China. China CDC Weekly 2(2): 19.

Ma T, Feng Y, Lin XF, et al. (2014). Psilocybe chuxiongensis, a new bluing species from subtropical China. Phytotaxa 156(4): 211–220. https://doi.org/10.11646/phytotaxa.156.4.3

Maire R (1933). Fungi Catalaunici. Contributions à l'étude de la flore mycologique de la Catalogne. Publicacions del Museu de Ciències Naturals de Barcelona, Sèrie Botànica 2: 3–120.

Malysheva E, Moreno G, Villarreal M, et al. (2019). The secotioid genus Galeropsis (Agaricomycetes, Basidiomycota): a real taxonomic unit or ecological phenomenon? Mycological Progress 18(6): 805–831. https://doi.org/10.1007/s11557-019-01490-6

Matheny PB, Liu YJ, Ammirati JF, et al. (2002). Using RPB1 sequences to improve phylogenetic inference among mushrooms (Inocybe, Agaricales). American Journal of Botany 89(4): 688–698. https://doi.org/10.3732/ajb.89.4.688

McTaggart AR, McLaughlin S, Slot JC, et al. (2023). Domestication through clandestine cultivation constrained genetic diversity in magic mushrooms relative to naturalized populations. Current Biology 33(23): 5147–5159. https://doi.org/10.1016/j.cub.2023.10.059

Meyer M, Slot, J (2023). The evolution and ecology of psilocybin in nature. Fungal Genetics and Biology 167: 103812. http://dx.doi.org/10.2139/ssrn.4384673

Miller MA, Pfeiffer W, Schwartz T (2010) Creating the CIPRES Science Gateway for inference of large phylogenetic trees. In: Proceedings of the 2010 Gateway Computing Environments Workshop (GCE): 1–8. IEEE.

Miller DR, Jacobs JT, Rockefeller A, et al. (2024) Cultivation, chemistry, and genome of Psilocybe zapotecorum. Journal of Psychedelic Studies 8(1): 63–81. https://doi.org/10.1556/2054.2023.00332

Minh BQ, Hahn MW, Lanfear R (2020). New methods to calculate concordance factors for phylogenomic datasets. Molecular Biology and Evolution 37(9): 2727–2733. https://doi.org/10.1093/molbev/msaa106

Morera G, Kuhar F, Rodriguez L, et al. (2024). A new species and new records of dung-associated bolbitiaceous fungi (Bolbitiaceae, Basidiomycota) from Uruguay. Phytotaxa 678(2): 109–124. https://doi.org/10.11646/phytotaxa.678.2.2

Nguyen LT, Schmidt HA, Von Haeseler A, et al. (2015). IQ-TREE: a fast and effective stochastic algorithm for estimating maximum-likelihood phylogenies. Molecular Biology and Evolution 32(1): 268–274. https://doi.org/10.1093/molbev/msu300

Niveiro N, Albertó EO (2012). Checklist of the argentine Agaricales 2. Coprinaceae and Strophariaceae. Mycotaxon 120(505): 74–86.

Nkadimeng, SM, Nabatanzi A, Steinmann CM, et al. (2020). Phytochemical, cytotoxicity, antioxidant and anti-inflammatory effects of Psilocybe natalensis magic mushroom. Plants 9(9): 1127. https://doi.org/10.3390/plants9091127

Noordeloos ME (2011). Strophariaceae s.l. Fungi Europaei 13. Edizioni Candusso, Saronno.

Ola'h GM (1969). Le genre Panaeolus: Taxonomic and physiologic essay. Revue de Mycologie, Mémoire Hors-Série 10: 1–273.

Ostuni S, Rockefeller A, Jacobs J, et al. (2024). Psilocybe niveotropicalis: a new species of psilocybin containing mushroom from South Florida. McIlvainea 33.

Ott J (1993). Pharmacotheon: Entheogenic Drugs, Their Plant Sources and History. Natural Products Co., Kennewick, Washington.

Persoon CH (1801). Synopsis methodica fungorum: sistens enumerationem omnium huc usque detectarum specierum, cum brevibus descriptionibus nec non synonymis et observationibus selectis. Vol. 2. Henrici Dieterich, Göttingen.

Plazas E, Faraone N (2023). Indole Alkaloids from Psychoactive Mushrooms: Chemical and Pharmacological Potential as Psychotherapeutic Agents. Biomedicines 11(2): 461. https://doi.org/10.3390/biomedicines11020461

Primo AT (1992). El ganado bovino ibérico en las Américas: 500 años después. Archivos de Zootecnia 41(154): 13.

Quélet L (1872). Les champignons du Jura et des Vosges. Imprimerie et lithographie de H. Barbier, Montbéliard.

Raison C (2019). A study of psilocybin for major depressive disorder (MDD). ClinicalTrials.gov. Available at: https://clinicaltrials.gov/ct2/show/NCT03866174

Ramírez-Cruz V, Guzmán G, Villalobos-Arámbula AR, et al. (2013). Phylogenetic inference and trait evolution of the psychedelic mushroom genus Psilocybe sensu lato (Agaricales). Botany 91(9): 573–591. https://doi.org/10.1139/cjb-2013-007

Richardson M.J (2001). Diversity and occurrence of coprophilous fungi. Mycological Research 105: 387–402. https://doi.org/10.1017/S0953756201003884

Robledo GL, Palacio M, Urcelay C, et al. (2020). Mystery unveiled: Diacanthodes Singer–a lineage within the core polyporoid clade. Systematics and Biodiversity 18(6): 538–556. https://doi.org/10.1080/14772000.2020.1776784

Robledo GL, Nakasone KK, Ortiz-Santana B (2021). Bjerkandera carnegieae comb. nov.(Phanerochaetaceae, Polyporales) a wood-decay polypore of cactus. Plant and Fungal Systematics 66(2): 230–239. https://doi.org/10.35535/pfsyst-2021-0021

Rodríguez L, Morera G, Lupo S, et al. (2025). Novel qNMR Method to Quantify Psilocybin and Psilocin in Psychedelic Mushrooms. ACS Omega 10 (46): 55725–55732 https://doi.org/10.1021/acsomega.5c07092

Ronquist F, Teslenko M, Van Der Mark P, et al. (2012). MrBayes 3.2: efficient Bayesian phylogenetic inference and model choice across a large model space. Systematic biology 61(3): 539–542. https://doi.org/10.1093/sysbio/sys029

Rosa-Mato F (1939). Agaricales del Uruguay. Physis 15: 123–127.

Saccardo PA (1887). Sylloge Fungorum omnium hucusque cognitorum. Vol. 5. Typis Seminarii, Patavii.

Schäfer T, Haun F, Rupp B, et al. (2025). Dissimilar Reactions and Enzymes for Psilocybin Biosynthesis in Inocybe and Psilocybe Mushrooms. Angewandte Chemie International Edition 64(46): e202512017. https://doi.org/10.1002/anie.202512017

Schröter J (1926). Panaeolus foenisecii sensu (Pers.). Botaniste 17(1–4): 187.

Senn-Irlet B, Nyffenegger A, Brenneisen R (1999). Panaeolus bisporus—an adventitious fungus in central Europe, rich in psilocin. Mycologist 13(4): 176–179.

Sequeira A (2013). Hongos: guía visual de especies en Uruguay. Ediciones de la Plaza.

Sequeira A (2017). Hongos silvestres comestibles en Uruguay. Ediciones de la Plaza.

Silva PSD (2013). Os gêneros Deconica (WG Sm.) P. Karst. e Psilocybe (Fr.) P. Kumm.(Agaricales) na região Sul do Brasil: contribuição á sua filogenia com bases morfológicas, moleculares e químicas. http://hdl.handle.net/10183/78755

Silva-Filho AG, Seger C, Cortez VG (2018). The neurotropic genus Copelandia (Basidiomycota) in western Paraná State, Brazil. Revista Mexicana de Biodiversidad 89(1): 15–21.

Silva-Filho AGS, Seger C, Cortez VG (2019). Panaeolus (Agaricales) from Western Paraná state, South Brazil, with a description of a new species, Panaeolus sylvaticus. Edinburgh Journal of Botany 76(2): 297–309. https://doi.org/10.1017/S0960428619000064

Singer R (1948). Diagnoses fungorum novorum Agaricalium. Sydowia 2: 26–42.

Singer R (1960). Sobre algunas especies de hongos presumiblemente psicotrópicos. Lilloa 30: 117–127.

Singer R (1969). Mycoflora Australis. Beihefte zur Nova Hedwigia 29. J. Cramer, Lehre.

Singer R (1976). Amparoinaceae and Montagneaceae. Revue de Mycologie 40(1): 57–64.

Singer R (1986). The Agaricales in modern taxonomy. 4th revised edition. Koeltz Scientific Books, Koenigstein.

Singer R, Smith AH (1958). Mycological investigations on teonanácatl, the Mexican hallucinogenic mushroom. Part II. A taxonomic monograph of Psilocybe, section Caerulescentes. Mycologia: 50(2): 262–303.

Smith HA (1948). Studies on dark-spored agarics. Mycologia 40: 669–707.

Stijve T (1995). Worldwide occurrence of psychoactive mushrooms-and update. Ceská Mycol 48: 11–19.

Stijve T, Demeijer A (1993). Macromycetes from the State of Paraná, Brazil. 4. The psychoactive species. Arquivos de Biologia e Tecnologia 36(2): 313–329.

Strauss D, Ghosh S, Murray Z, et al. (2022). An overview on the taxonomy, phylogenetics and ecology of the psychedelic genera Psilocybe, Panaeolus, Pluteus and Gymnopilus. Frontiers in Forests and Global Change 5: 813998. https://doi.org/10.3389/ffgc.2022.813998

Strauss D, Ghosh S, Murray Z, et al. (2023). Global species diversity and distribution of the psychedelic fungal genus Panaeolus. Heliyon 9(6): e16338. https://doi.org/10.1016/j.heliyon.2023.e16338

Tóth A, Hausknecht A, Krisai-Greilhuber I, et al. (2013). Iteratively refined guide trees help improving alignment and phylogenetic inference in the mushroom family Bolbitiaceae. PLoS ONE 8(2): e56143. https://doi.org/10.1371/journal.pone.0056143

Van Der Merwe B, Rockefeller A, Kilian A, et al. (2024). A description of two novel Psilocybe species from southern Africa and some notes on African traditional hallucinogenic mushroom use. Mycologia 116(5): 821–834. https://doi.org/10.1080/00275514.2024.2363137

Van Court RC, Wiseman MS, Meyer KW, et al. (2022). Diversity, biology, and history of psilocybin-containing fungi: Suggestions for research and technological development. Fungal Biology 126(4): 308–319.https://doi.org/10.1016/j.funbio.2022.01.003

Velenovský J (1930). Galeropsis gen. nov. Mycologia 7: 105–106.

Vilgalys R, Hester M (1990). Rapid genetic identification and mapping of enzymatically amplified ribosomal DNA from several Cryptococcus species. Journal of Bacteriology 172(8): 4238–4246. https://doi.org/10.1128/jb.172.8.4238-4246.1990

Voto P, Angelini C (2021). First record of Copelandia mexicana in Dominican Republic and notes on Panaeolus. Mycological Observations 1: 44–58.

Voto P, Angelini C (2024). Studies in the Panaeolus papilionaceus complex (Agaricales, Galeropsidaceae): two new species discovered in the Dominican Republic and Australia. Mycological Observations 9: 1–32.

Wang YW, Tzean SS (2015). Dung-associated, Potentially Hallucinogenic Mushrooms from Taiwan. Taiwania 60(4): 160–168. https://doi.org/10.6165/tai.2015.60.160

Wasson RG (1957). Seeking the magic mushroom. Life 42(19): 100–120.

White TJ, Bruns T, Lee S, et al. (1990). Amplification and direct sequencing of fungal ribosomal RNA genes for phylogenetics. In: PCR Protocols: A Guide to Methods and Applications (Innis MA, Gelfand DH, Sninsky JJ, White TJ, eds). Academic Press, San Diego: 315–322.

Windsor C, Kreynes AE, Chilton JS, et al. (2025). Development of Psilocybe Mushroom Species Reference Material—Cultivation Parameters and Chemical Profiles. Journal of AOAC International 109(1): 37–50. https://doi.org/10.1093/jaoacint/qsaf007

Wright JE, Albertó E (2002). Hongos: guía de la Región Pampeana. Vol. 1. Hongos con laminillas. LOLA.

Young AM (1989). The Panaeoloideae (Fungi, Basidiomycetes) of Australia. Australian Systematic Botany 2(1): 75–97. https://doi.org/10.1071/SB9890075

Zhuk O, Jasicka-Misiak I, Poliwoda A, et al. (2015). Research on acute toxicity and the behavioral effects of methanolic extract from psilocybin mushrooms and psilocin in mice. Toxins 7(4): 1018–1029. https://doi.org/10.3390/toxins7041018

Supplementary Material: http://fuse-journal.org/

Supplementary material

Table S1. Sequences of *Panaeolus* species used in the phylogenetic analyses. New sequences generated in this study are highlighted in bold. An emdash (—) indicates missing data.

Table S2. Sequences of *Psilocybe* species used in the phylogenetic analyses. New sequences generated in this study are highlighted in bold. An emdash (—) indicates missing data.